A pre-LGM sandur deposit at Fiskarheden, NW Dalarna - sedimentology and glaciotectonic deformation

Anne-Cécile Flindt

Dissertations in Geology at Lund University,
Master's thesis, no 463
(45 hp/ECTS credits)

Department of Geology
Lund University
2016

A pre-LGM sandur deposit at Fiskarheden, NW Dalarna - sedimentology and glaciotectonic deformation

Master's thesis

Anne-Cécile Flindt

Department of Geology
Lund University

2016

Contents

Cover Picture *(taken by A-C Flindt)*: Icelandic braided river system fed by a close active glacier, such as what Fiskarheden could have been like at the time of depostion.

A pre-LGM sandur deposit at Fiskarheden, NW Dalarna - sedimentology and glaciotectonic deformation

ANNE-CECILE FLINDT

Flindt, A.C., 2015: A pre-LGM sandur deposit at Fiskarheden, NW Dalarna – sedimentology and glaciotectonic deformation. *Dissertations in Geology at Lund University*, No. 463, 34 pp. 45 hp (45 ECTS credits)

Abstract: The Fiskarheden quarry, situated in NW Dalarna, central Sweden, reveal thick deposits of coarse-grained sediments of Scott type facies association; a sandur deposited in an ice-proximal proglacial environment. Preliminary OSL dating of the sandur sediments suggest that they are of a pre-Saalian age (>200 000 years). Of special interest here is, besides its pre-LGM age, the large-scale and intense glaciotectonic deformation of the sediments. Both ductile folding and brittle deformation structures suggest glacial stress from NW which coincides with the trend of surrounding streamlined terrain and to that trend perpendicular Rogen moraine. From sedimentological relations and the glaciotectonic architecture it is suggested that either (i) the deformation of the sandur sediments took place when the glacier approached and overrode its own proglacial meltwater sediment, or that (ii) the deformation is from a younger ice advance over the area, decoupled from the deposition of the sandur sediments. The Fiskarheden sandur deposits are covered by traction till deposited from NE/NNE. This direction conforms to younger cross-cutting streamlined terrain to the older NW-SE system and is suggested to represent the LGM deglaciation phase over the area.

Keywords: glaciotectonic, glaciofluvial, sandur, structures, deformation, fault-propagation fold.

Supervisor: Per Möller

Subject: Quaternary Geology

Anne-Cécile Flindt, Department of Geology, Lund University, Sölvegatan 12, SE-223 62 Lund, Sweden. E-mail: flindtannececile@yahoo.fr

En sanduravlargring vid Fiskarheden i nordvästra Dalarna av pre-LGM ålder – sedimentologi och glacialtektonik

FLINDT ANNE-CÉCILE

Flindt, A.C., 2015: En sanduravlargring vid Fiskarheden i nordvästra Dalarna av pre-LGM ålder – sedimentologi och glacialtektonik. *Examensarbeten i geologi vid Lunds universitet*, Nr. 463, 34 sid. 45 hp.

Sammanfattning: Ett grustag vid Fiskarheden, som ligger i nordvästra Dalarna, uppvisar tjocka avlagringar av grovkorniga sediment; en sanduravlagring av så kallad Scott-typ som deponerats i en is-proximal proglacial miljö. Preliminära OSL-dateringar av sandursedimenten tyder på att de är av en pre-Saalian ålder (>200 000 år). Av särskilt intresse här är, förutom dess höga ålder pre-daterande det senaste istidsmaximat, storskalig och intensiv glacialtektonisk deformation av sedimenten. Både plastiska och spröda deformationsstrukturer tyder glacialt tryck från nordväst, vilket sammanfaller med riktningen av omgivande strömlinjeformad terräng och från den trenden vinkelräta Rogenmoräner. Från sedimentologiska relationer och glacialtektonisk arkitektur föreslås att deformation av sanduravlagringen inträffade (i) antingen när glaciären närmade sig och överskred sina egen proglacial smältvattensediment, eller att (ii) deformationen är från ett yngre isöverskidande över området, frikopplat från deponerings av sandursediment. Fiskarhedens sandursediment är täckta av morän avsatt från NO till NNO. Denna riktning överensstämmer med yngre strömlinjeformat terräng som skär över det yngre NV mot SO-systemet av strömlinjeformer. Denna morän föreslås representera avsmältningsfasen av inlandsisen från den senaste glaciationen över området.

Nyckelord: glacialtektonik, glacifluvial, sandur, strukturer, deformation

Anne-Cécile Flindt, Geologiska institutionen, Lunds Universitet, Sölvegatan 12, 223 62 Lund, Sverige. E-post: flindtannececile@yahoo.fr

1. Introduction

Fennoscandia has been glaciated repeatedly during the Quaternary; various parts of Northern Europe were covered by up to four times with deglaciation in between during only the last glacial cycle, the Weichselian (Mangerud *et al*. 2011). It has for long been regarded that the landscape of Fennoscandia was formed during the last deglaciation. A paradigm shift happened in the 90s when it was realized that many landforms, especially in the northern part of Sweden were formed during earlier glaciations/deglaciation, and especially from the Early Weichselian. These regions were suggested to have been preserved beneath cold based ice during later glacial over-riding (e.g. Ljungner 1949; Lagerbäck 1988a, b; Lagerbäck & Robertsson 1988; Kleman *et al*. 1997; Kleman & Stroeven 1997; Kleman & Hättestrand 1999; Kleman & Glasser 2007) and considered to have been covered by ice from *Marine Isotope Stage* 4 (MIS 4), over MIS 3 and into the last Glacial Maximum (LGM), i.e. over a time period of c. 80 to 10 ka BP (e.g. Mangerud 1991a, b).

Sites with exposed sediments beneath the surface till are generally not many in Sweden. However, central parts of Sweden, especially the counties of Dalarna and Jämtland, hosts a large number of these sub-till sorted sediment successions. These have in the last years gathered much interest, especially as new dating techniques have been introduced. Recently found sites, together with reinvestigated and re-dated stratigraphic records from previously well-known sites in central and northern Sweden as well as in Finland, have opened up for new interpretations about the glacial history. Instead of an ice cover over central to northern Fennoscandia during the whole of MIS 3 (c. 60-11.7 ka BP), much evidence now points towards deglaciation of these areas during parts of MIS 3 before ice started to form again, leading to the LGM glaciation (Helmens 2009; Helmens *et al.* 2000, 2007; Hättestrand 2007; Ukkonen *et al.* 2007; Lunkka *et al*. 2008, 2015; Salonen *et al*. 2008; Alexanderson *et al*. 2010; Helmens & Engels 2010; Hättestrand & Robertsson 2010; Wohlfarth 2010; Wohlfarth & Näslund 2010; Wohlfarth *et al.* 2011; Möller *et al.* 2013).

The till cover over west central Sweden is usually considered to be from the LGM glaciation/ deglaciation. Sub-till sediments of various types are therefore presumably pre-LGM deposits, meaning interstadial/interglacial ice-free conditions strata or proglacial inception phase/deglacial phase sediments from earlier glaciations (Möller *et al*. 2013). The Fiskarheden site in NW Dalarna (Fig. 1) is such a site with a thick sequence of clastic, coarse-grained sorted sediment beneath a covering till, but a site that has been close to non-investigated except for a minor reconnaissance study made by the Geological Survey of Sweden (SGU) (Svedlund 2005). Of special interest here are, besides the pre-LGM age of the sorted sediment, the large-scale glaciotectonics revealed at site. The aims of this work are two-fold; (i) to document and interpret the primary deposition of the sub-till sorted sediment succession and (ii) to document the tectonic structures and their relation to the covering till, all with a goal to reconstruct the glacial history of the area. As will be seen the sorted sediment succession is interpreted as a proglacial sandur deposits that has undergone considerable glaciotectonic deformation. This paper thus starts with a literature review of braided river outwash systems and back-ground fundamentals on glaciotectonics

2. Literature review

2.1. Braided river systems

Braided rivers have a multitude of river channels marked by "successive division and rejoining of the flow around alluvial islands" (Renineck & Singh 1975). Such can, however, form in a number of geological/geomorphological settings. According to Miall (1977) "glacial outwash streams are almost invariably braided". The network of braided rivers, often found in sandar systems, shapes distinctive signatures in the sedimentary record and its depositional area (Magilligan *et al.* 2002); forming an active system of bars and channels that fluctuates through time and, especially, with seasons (Miall 1977). In rivers, discharge variability will go along with competence variability, i.e. the ability to transport sediment. Rivers will therefore be unable to move the coarsest part of their bedload sediment for long time periods, allowing bar initiation, flow diversion and new channel creation (Miall 1977). Braided streams are usually signified by steep slopes and low sinuosity (Miall 1977), which contribute to high water flow dynamics. Thus there usually will be a low to nonexistent sedimentation of the finer sediment load upstream (the proximal part of the system), but with markedly decreasing grain size of deposited sediment in downstream direction (the distal part of the system).

The notions of proximal and distal sedimentation characteristics are thus very characteristic for braid-plain depositional systems. Several parameters are needed to provide an accurate but not 'absolute' indication of the proximity of the sediment source for braided river environments but, as Miall (1977) describes it, grain size is the most important indicator of them all. In the proximal part of the system coarser bed load sediments are dominant due to the high flow energy present, resulting in deposition of a predominance of gravelly to cobbly/ bouldery facies. The extent of the proximal coarse-grain sediment dominated reach of braided rivers can be up to 15–50 km (Williams & Rust 1969). Down-stream the flow energy decreases and therefore more fine-grained sediment start to dominate in the more distal parts of the system (Zielinski & van Loon 2003). However, lower flow-energy deposits might also, with varying frequencies, be preserved within the proximal system for many reasons; sediments deposited and preserved in main channels during low stages,

sediment infill in side/secondary channels with lower flow discharges, or scour-pool and bar-edge aggradation (Miall 1977; Zielinski & van Loon 2003). Bars often create sideways/reverse flows towards their lee sides with back pool and lee-side accumulation showing, e.g., planar laminated to ripple laminated sands (Miall 1977).

Outwash aggradation systems have been described by many authors (e.g., Williams & Rust 1969; Rust 1972; Boothroyd & Ashley 1975; Miall 1977) and general facies models of braid-plain depositional systems have been erected (Miall 1977). Facies assemblages typical of proximal settings, the Scott and Trollheim facies models (Miall 1977), in which sediment supply is large relative to water discharge, are dominated by stacking of debris flows or multiple sets of coarse clast-supported gravel/ cobble/boulder during bar aggradation at high stages, and bar-edge and lee-side deposition during lower-flow stages (Miall 1977; Benn & Evans 2010). As the bar is aggrading and slightly prograding, the finer-grained bar-edge and lee-side sediments will show interfingering with the surroundings bar deposits (Miall 1977; Zielinski & van Loon 2003) and are accordingly interpreted to be preserved sediments from lee side scours of longitudinal bars.

In facies assemblages typical of intermediate and distal settings, the Donjek and the Platte facies models, respectively (Miall 1977), grain-sizes of deposited sediments are in average smaller compared to proximal settings. The Donjek type can also reveal different topographic levels due to abandonment of the braid channels most of the time, all channels only inundated during high flow stages. Bedforms typical for the intermediate Donjek facies model are stacked channel fill sequences of planar and trough cross sand to gravelly sand (deposited due to migration of 2D and 3D dunes, planar lamination and ripple cross-lamination) (Miall 1977; Benn & Evans 2010).The Platte facies model is typical of distal settings. It is dominated, due to a lower sediment supply relative to the water discharge, by sandy bedforms with abundant cross-beddings (Miall 1977; Benn & Evans 2010).

Sediment distribution over a braidplain depends mainly on the morphology of the proglacial fluvial system. As discussed above, the flows' dispersion, the bars' accretion and the overall shift in the system due to energy fluctuations allow specific sedimentary features within braided systems (Zielinski & van Loon 2003). Main and secondary channels have different conditions and styles of sedimentation, channel stability and bed load transport (Nicholas & Sambrook Smith 1998). These constant flow shiftings complicate the overall picture and, as pointed out by Zielinski & van Loon (2003), 'as a rule, braided channels are shallow and during phases of waning flood shoaling takes place'. In secondary channels present in the proximal part of a braid-plain system, during waning flow periods, sandy facies might be deposited and preserved in an environment where coarser materials usually dominate.

2.2. Glaciotectonism and glacier motion

A glaciers' ability to move is a fundamental characteristic. Studies on the behavior and physics of glacier motion drove intense questioning for some two centuries. But obtaining information within and below a glacier has been difficult until recently with the introduction of modern advanced techniques such as, e.g., powerful radar scanning, seismic analyses, GPS recording and numerical modeling, which all have allowed more difficult location in the glacier to be measured (Benn & Evans 2010). However, even with these new techniques there is a lot that is still unknown about glaciodynamics.

Apart from the motion of glaciers due to englacial deformation of the ice crystals and basal sliding, sediments beneath the ice/bed interface can take part of this motion, in the extreme case as a total mobile bed that moves along with the glacier, either above a décollement plane (a shear surface) at varying depth beneath that interface, or as a bed with gradual decrease in its deformation downwards, concepts introduced by, e.g., Boulton (1982, 1987) and Boulton & Hindmarsh (1987). Deformed subglacial sediment can be totally obliterated of their original structures if this deformation is totally penetrative, transforming the sediment into a massively deformed, i.e. massive structure, sediment (e.g. a deformation till; Benn & Evans 2010). However, if deformation stops before the total obliteration of original structures, the mode and scale of deformation can possibly be deduced from the sediment, and recognized as glaciotectonic structures.

Glaciotectonism has clearly multiple possible settings. It can take place beneath a glacier, in front of an ice sheet margin or at the margin itself. Many factors can be associated to glaciotectonic deformations, such as regional and local topography, substratum composition, pore water pressure, and cold - or warm-based basal regimes (Aber *et al.* 1989; Benn & Evans 2010). These patterns may potentially be important for geologic work and can evolve within shorter or longer time frames and/or over smaller or larger distances along a flow line (Aber *et al.* 1989).

Stress and strain are two concepts that have clear meanings when it comes to glaciotectonic deformation. 'Stress', especially effective normal stress (i.e. total stress minus pore water pressure) is the force applied over an area from a glacier, while 'strain' represents the total amount of deformation induced by that stress (Benn & Evans 2010), while strain rate is deformation over time unit. The stress induced by glaciers need to exceed the shear strength of the sediment at or below the ice-bed interface for the material to be deformed and glaciotectonic structures to appear. There are a number of parameters that need to be considered in order to complete a stress-strain analysis of recognized glaciotectonics.

Two kinds of stresses can be transferred by a glacier to its substratum: (i) glaciostatic pressure and, (ii) glaciodynamic stress. The glaciostatic pressure is induced by the vertical pressure of ice, whereas the

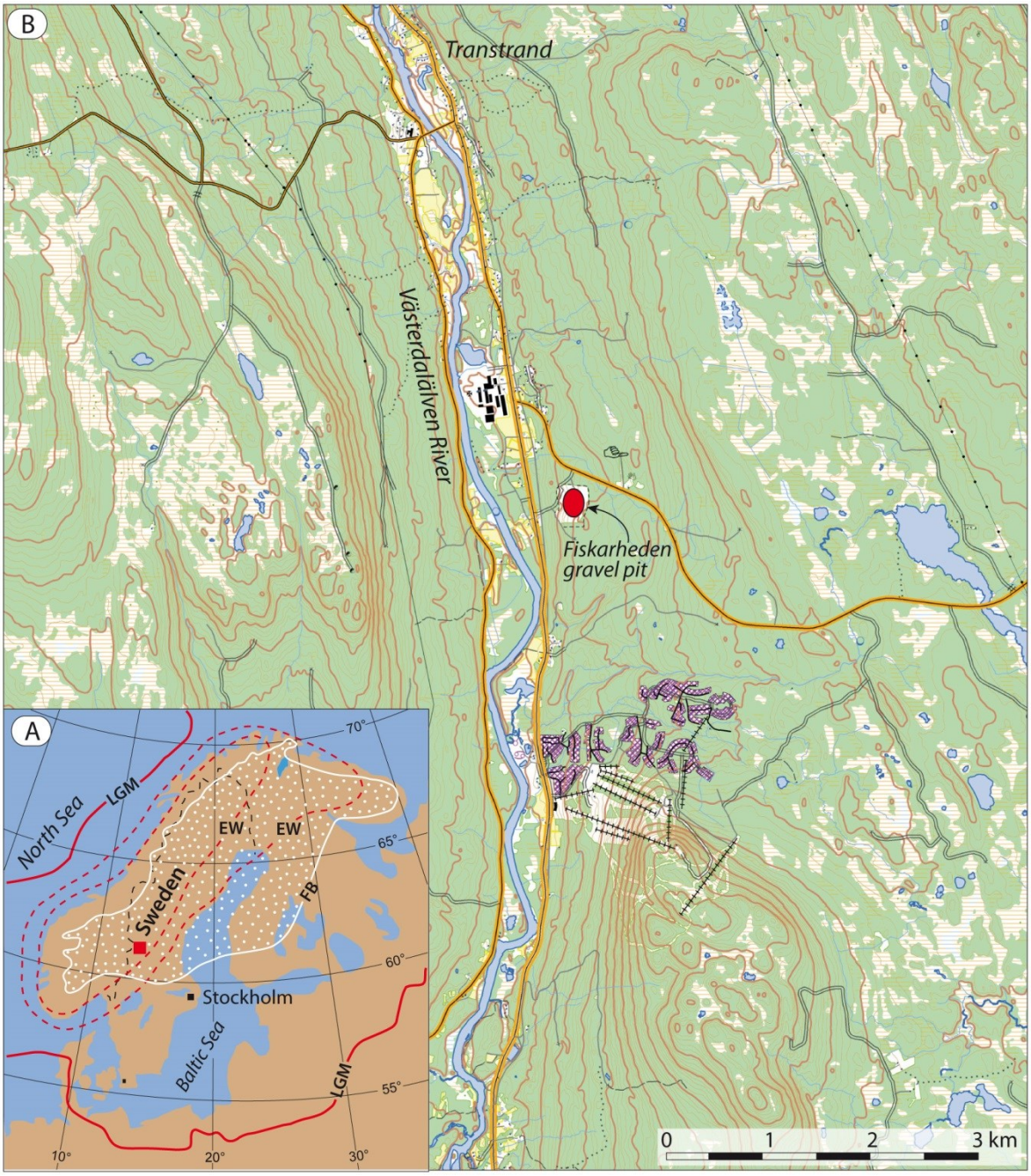

Fig. 1. (A) Overview map. Fennoscandia with schematic ice-sheet outlines for the Late Weichselian Maximum (LGM) and Early Weichselian (EW), adopted from Kleman et al. (1997). White-dotted area within boundary marked FB shows the minimum extent of frozen-bed conditions during the LGM according to Kleman et al. (1997) (entirely taken from Möller et al. 2013). The position of the Fiskarheden area (not to scale) is marked with a red square. (B) Topographic map over the Fiskarheden – Transtrand area. The red dot marks the Fiskarheden gravel pit. Map data provided by Lantmäteriverket, Sweden; ©Lantmäteriverket i2012/927.

glaciodynamic stress is introduced by the ice movement over the ice-bed interface ($\tau_b = \sigma_x * \sin \alpha$), irrespectively of the glacier margin is advancing or retreating (Aber *et al*. 1989). A lateral pressure component is formed by the glaciostatic pressure; as ice thickness is gradually decreasing towards the ice margin this pressure build a lateral stress gradient ($\Sigma D\sigma_x$) that increases towards the ice margin, independently of ice displacement due to drag or shear over that bed (Aber *et al.* 1989). These together build the total glaciotectonic stress ($\sigma_{gt} = \Sigma D\sigma_x + \tau_b$). In fact, as expressed by many authors (Rotnicki 1976; van der Wateren 1985; Aber *et al.* 1989; Williams *et al.* 2001) and what is often concluded from field work, glaciotectonics are most likely to develop at the ice margin where the ice has the steepest gradient and hence the highest lateral pressure gradient.

The combined stress impact on the ice bed tends to create a substratum disturbance. Due to the shear stress from above (τ_b), a surface of décollement

is commonly initiated at a weaker layer or a weaker bed within the substratum located below the ice-bed interface. This surface can almost be qualified as the 'root of the deformation' to put it simply. It is usually localized below a glaciotectonically, marginally stacked system and not often identified in the field. However, its previous location can be calculated according to, e.g., Benediktsson *et al*. (2010).

Marginal and subglacial glaciotectonic structures are the most frequently observed features of ice deformation (Madsen & Piotrowsky 2012). It usually shows up as stacked sediment packs along a series of medium angled thrusts (± 30°) (Aber *et al*. 1989). Commonly, thrust faults occur at surfaces of maximum shear stress in cohesive materials, which is surfaces with an inclination of 45° towards the stress direction, while faulting occur along surface with lower inclination (down to 30°) in frictional sediment. Glaciotectonic structures are confined in three different systems, (i) the ductile system, (ii) the ductile -fragile system and, (iii) the fragile system (Hart & Boulton 1991; van der Wateren 1985; Williams *et al*. 2001); all three systems have been identified within the sediments exposed at Fiskarheden, which will be shown later.

Before the 1980's, 'soft sediments' where taken under little consideration when it comes to ice motion (Benn & Evans 2010). Later, researchers as, e.g., Boulton (1979), Boulton & Jones (1979), Boulton & Hindmarsh (1987), Alley *et al.* (1986) and Blankenship *et al.* (1986) have discussed unlithified and water saturated substrata's role in control of ice motion, as well as different deformation scenarios. Hart and Boulton (1991) also put into perspective the possible correlation between general structural geology (tectonics) and glaciotectonics. They pointed out that glaciotectonic structures could very well represent 'a natural scale-model of the low aspect ratio ('thin-skinned') tectonics observed in hard rock thrust belts, such as the Appalachians and the Helvetic Alps (Banham 1988; Croot 1987). Consequently, qualitative comparisons of glaciotectonic structures with large-scale geologic structures in bedrock may be applicable (Croot 1987). However, some important differences between metamorphic shear zones and subglacial shear zones must be made. Within metamorphic deformations, masses are 'passively' deformed. In glacial environments the glacier might interact and give some 'outside input'. The nature of the deformation might therefore go through changes over time, especially when ice in motion interacts with its substratum (Hart & Boulton 1991).

In Brandes & Le Heron (2010), the fault-propagation-folding and the trishear kinematic models suggest an interesting approach, building on the kink-fold model from Suppe and Medwedeff (1990). To put it simply, a shear zone where simple shear occurs is a narrow zone between two sub-horizontal walls (Hobbs *et al.* 1976; Ramsay & Graham 1970; Tikoff & Fossen 1993; Hardy & Poblet 1995). In a glacial environment, the top 'wall' is the ice-bed interface and the bottom of the shear zone an undeforming substratum. As an analogue, a shear zone in 'hard rock', mainly found within metamorphic environments, is identified by mylonitic (Ramsay & Graham 1970) or/and by cataclastic zones (Lapworth 1885; Spry 1969; Hobbs *et al*. 1976). Such zones produce a so called 'fault flour' of their adjacent surrounding rocks due to their brittle crushing which give numerous deformational parameters, such as direction and sense of shearing.

For clarity aspects and to aid the reader to follow the technical glaciotectonic terms, Fig. 2 shows described and discussed structures at Fiskarheden as in simplified cartoons. The structural elements description is based on three types of deformation: ductile deformation (A), brittle deformation (B, C) and brittle-ductile deformation and tectonic structures (D) as used in this work (basic approach according to Pomerol *et al.* (2008) and Benn & Evans (2010)).

3. Regional setting

As presented above, the county of Dalarna is well known for being a key area in which to observe and understand paleo-indicators for supposedly east-west ice divide migrations (Ljunger 1949; J. Lundqvist 1969, 1986).

The Fiskarheden gravel pit is located in the Västerdalälven river valley in the NW part of Dalarna County (Fig. 1). Västerdalälven, flowing in a close to north towards south direction, is deeply incised in the mountainous area and is having an almost 1 km wide flood plain at c. 350 m above sea level. The valley sides rise to c. 600 m a.s.l. to the west of the valley, and to c. 520 m a.s.l. east of it. The highest mountains in the area are the Transtrand Mountains, c. 2 km towards the west, which rise to twenty summits between 850-950 m a.s.l.

The bedrock of the area mainly consists of Precambrian (Jotnian) sandstones with nearly horizontal bedding (Hjelmqvist 1966; Kleman *et al*. 1992), as well as isotropic ultrabasic, basic, intermediate and acid volcanic rocks (basalt, andesite, rhyolite, etc.; mainly Öje basalt) present in intrusive dykes and more spread intrusions.

The dominating Quaternary sediment (Fig. 3) in the area is till, sometimes thin as evident from quite large outcrops of bedrock, but also thicker such, which as shown from the DEM's (Figs. 5 and 6) takes form both as hummocky moraine, ribbed moraine and streamlined terrain. The drumlin ridges of the latter have NW-SE to almost N-S orientations. Glaciofluvial sediment is predominantly located in the Västerdalälven valley and its tributaries and glaciofluvial channels of varying widths are all converging towards the river valley. Peat covers large areas. At Fiskarheden is mapped glaciofluvial sediments covered by till, measuring c. 1 by 2 km.

The glacial history of the area, as so far known, has mainly been described by G. Lundqvist (1951), Kleman (1990) and Kleman *et al.* (1992). Kleman *et*

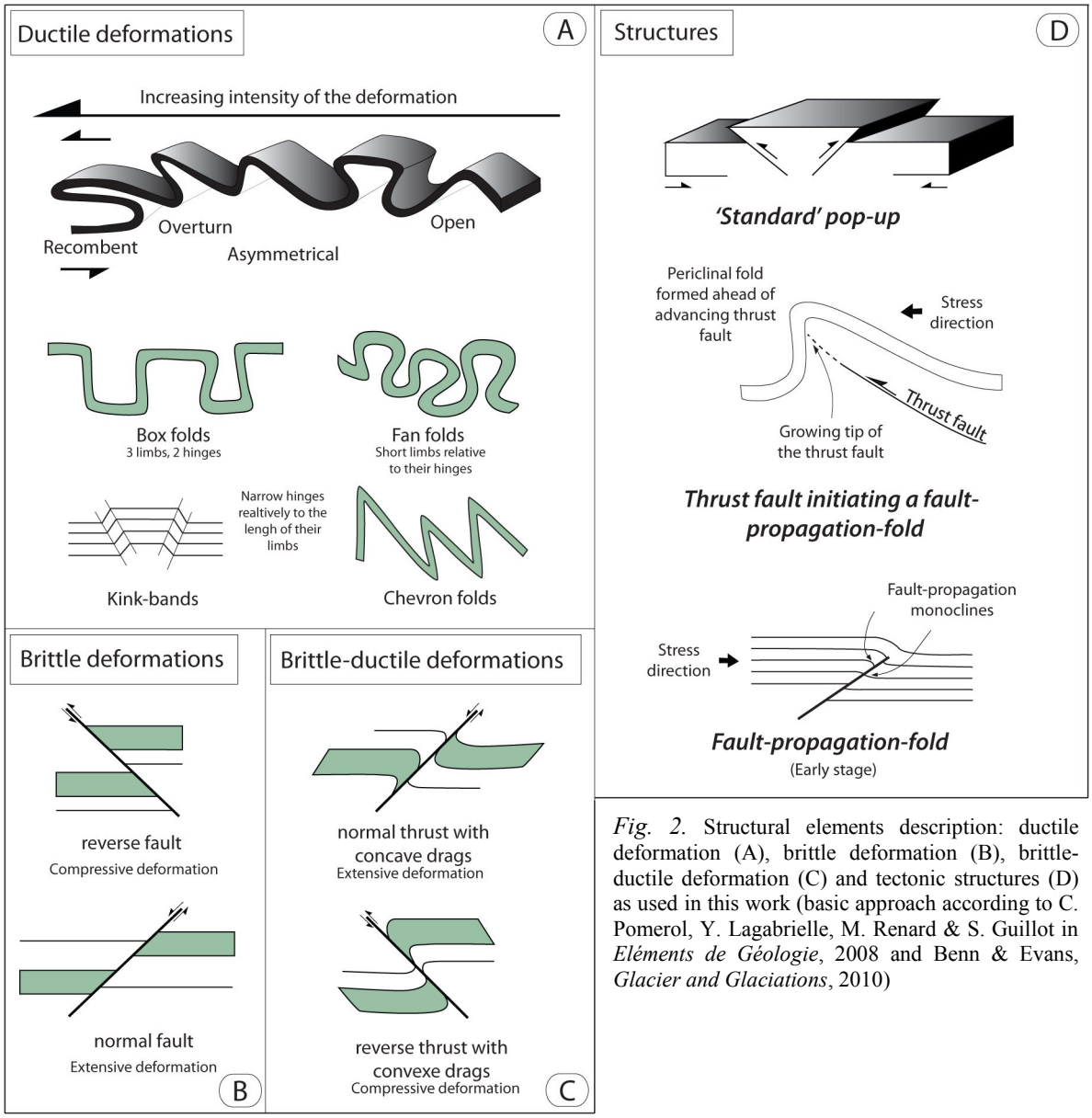

Fig. 2. Structural elements description: ductile deformation (A), brittle deformation (B), brittle-ductile deformation (C) and tectonic structures (D) as used in this work (basic approach according to C. Pomerol, Y. Lagabrielle, M. Renard & S. Guillot in *Eléments de Géologie*, 2008 and Benn & Evans, *Glacier and Glaciations*, 2010)

al. (1992) described glaciofluvial drainage channel sets over the Transtrand Mountains, often showing cross-cutting relations. These channel sets were formed parallel to the lateral ice margins of shrinking ice tongues and therefore indicate the lateral ice margin orientation at the time of the glaciofluvial incision, and thus the local ice flow direction, being parallel to the lateral channels. However, the discerned flow sets divide up in at least four such in very different directions. This suggests that they represent at least four different deglaciations over the area, of which three are older than the LGM deglaciation (Kleman *et al*. 1992). The youngest set of meltwater channels suggests an ice flow direction from NNE and thus an ice recession towards the same direction, tied to the LGM deglaciation. The second youngest channel set suggests an ice flow direction from NW-NNW, which is concordant with the predominant direction of streamlined terrain at the valley bottoms (see below). At trench digging over the channels, Kleman *et al*. (1992) recognized two tills ('yellow tills') older than the youngest till ('red till'). The latter has a fluted surface, suggesting an ice flow from north -northeast (i.e. the LGM ice-flow deglaciation direction over the area). The contact between the upper yellow till and the red till often showed gravel beds indicative of glaciofluvial activity, as also was the case between the two yellow tills. Furthermore, at one locality was a palaeosol at this contact, giving an infinite radiocarbon age of >45 ka BP.

According to Kleman (1990) the Transtrand area formed a melted bed patch at the last deglaciation, as suggested from glacial striae from N-NNE and basal till with a fluted surface on the Transtrand Mountains. Kleman (1990) argued that the main morphological elements in the area, NW-SE directed streamlined terrain (drumlins) and Rogen moraines perpendicular to that direction, and surrounding the Fiskarheden area with NE to SW ice-flow indicators, are incompatible with an ice flow direction that would prevailingly be from E-ENE with an LGM Fennoscandian Ice Sheet dome over the Gulf of

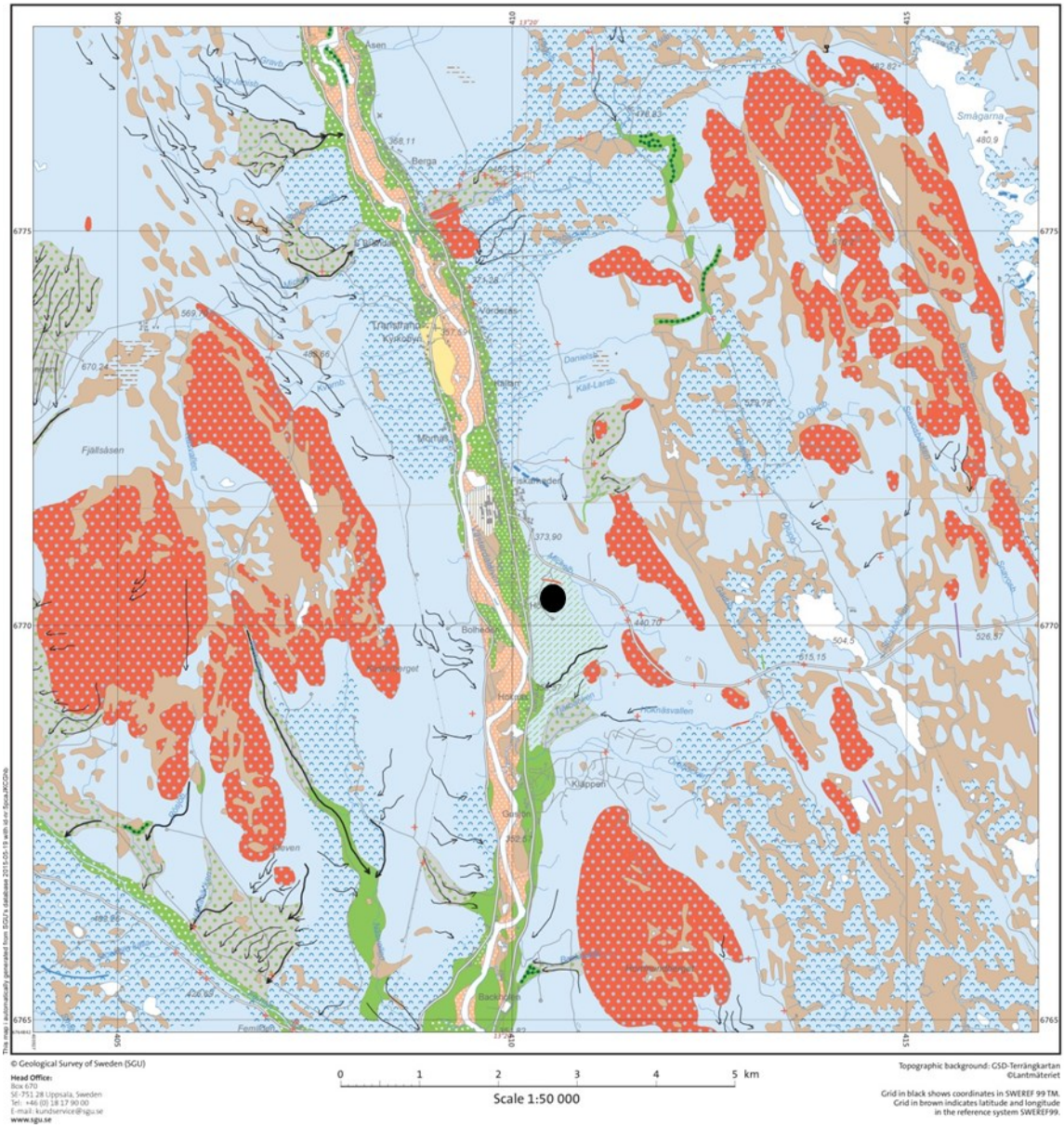

Fig. 3. Overview map. Quaternary cover map from the Swedish Geological Survey (SGU) showing the surroundings of Fiskarheden gravel pit site. The blue represent the till cover of the area, the red show bedrock knobs at the surface usually covered with a discontinuous thin till cover; the bright green shows glaciofluvial sediments; the light brow represents the peat cover. The blue symbols '^' express the hummocky moraine cover spread over the area and the black lines ending by an arrow represents glaciofluvial channel drainages. Fiskarheden quarry pit is symbolized by a black spot.

Bothnia, as argued by, e.g., Denton & Hughes (1981) and Boulton *et al.* (1985). As no striae or geomorphic landforms concur with such an ice-flow orientation, Kleman (1990) argued that the Fennoscandian ice sheet was frozen at its base over Dalarna at this time, and only became wet-based – but only over restricted areas – during deglaciation. Further, he suggested that the landforms indicating an ice flow from NW (the majority of drumlins and Rogen moraines) were formed either during the inception phase of the last glaciation, or from earlier glaciations, and preserved beneath cold-based ice.

4. Methods

The sediments exposed within the Fiskarheden gravel pit were studied along an approximately 19 m high, quite vertical, actively quarried back-wall in the pit (section sites 4-7, Fig. 4) as well as along a less high, non-quarried section remnant, left for reduction of noise towards nearby houses (section sites 1-3, Fig. 4). The diamict covering the gravel deposits was studied in a c. 4 m high section in the southeast part of the quarry where the diamict and a few meters of the underlying gravel had been removed behind the actively quarried section (site 9, Fig. 4), as well as within a machine-dug test pit, 3 m deep, dug down

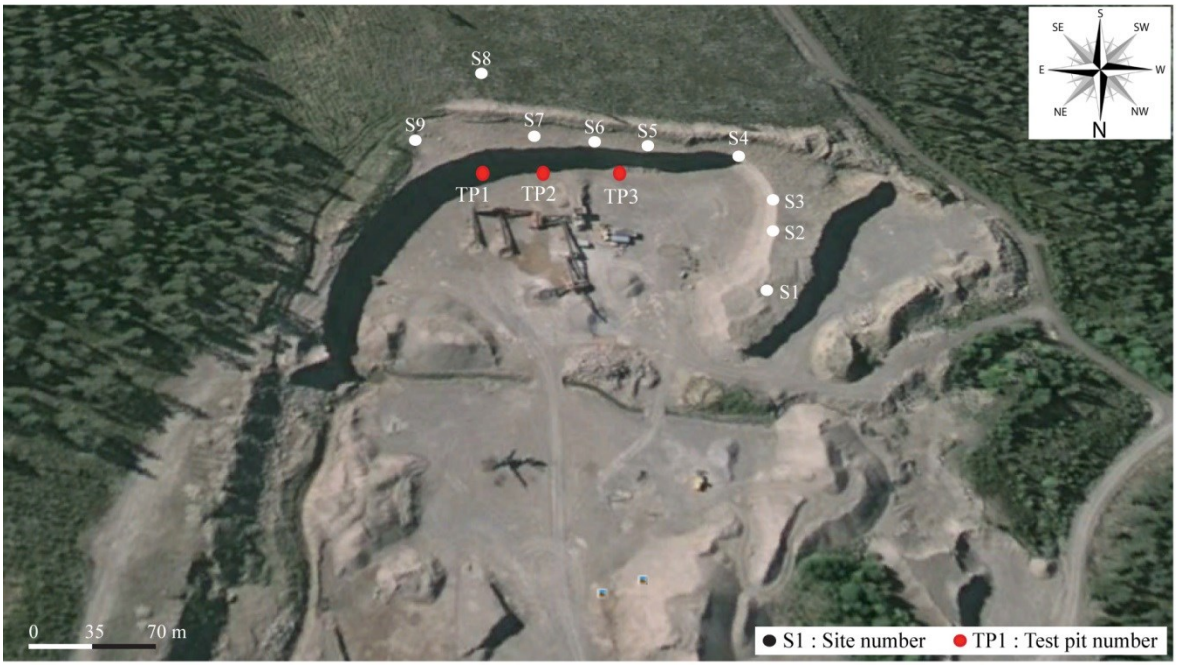

Fig. 4. Google Earth overview crop of the Fiskarheden pit and position of described sections are marked by white dots numbered S1-S9. Test pits in front of the main section wall are numbered TP1-3 and marked with red dots.

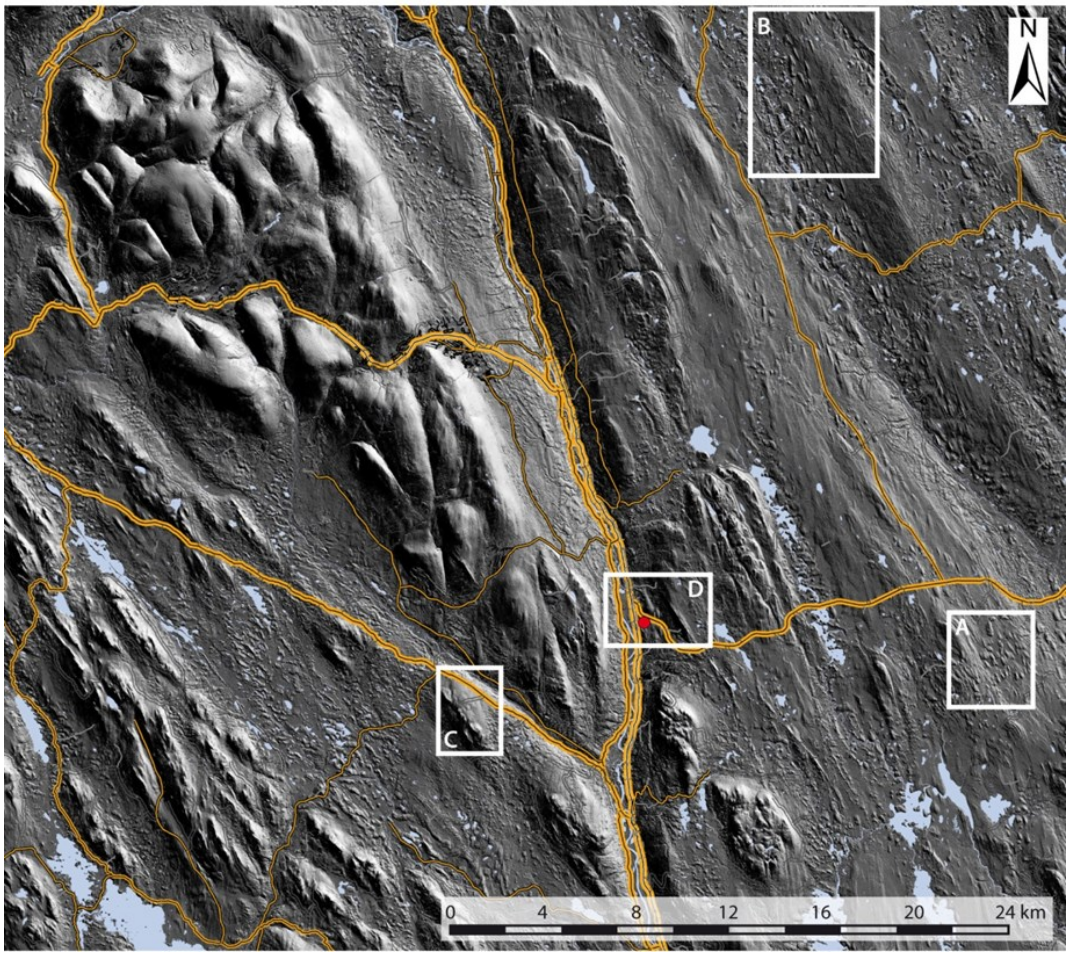

Fig. 5. Hill shade constructed from LiDAR scan data in the "New National Height Model" with a 0.1 m height and a 2*2 m width resolution (data provided by Lantmäteriverket, Sweden; ©Lantmäteriverket i212/927). The Fiskarheden gravel pit is indicated by red dot. White frames numbered A-D are selected areas demonstrating ice flow directions as indicated by streamlined terrain in larger-scale DEMs (Fig. 6).

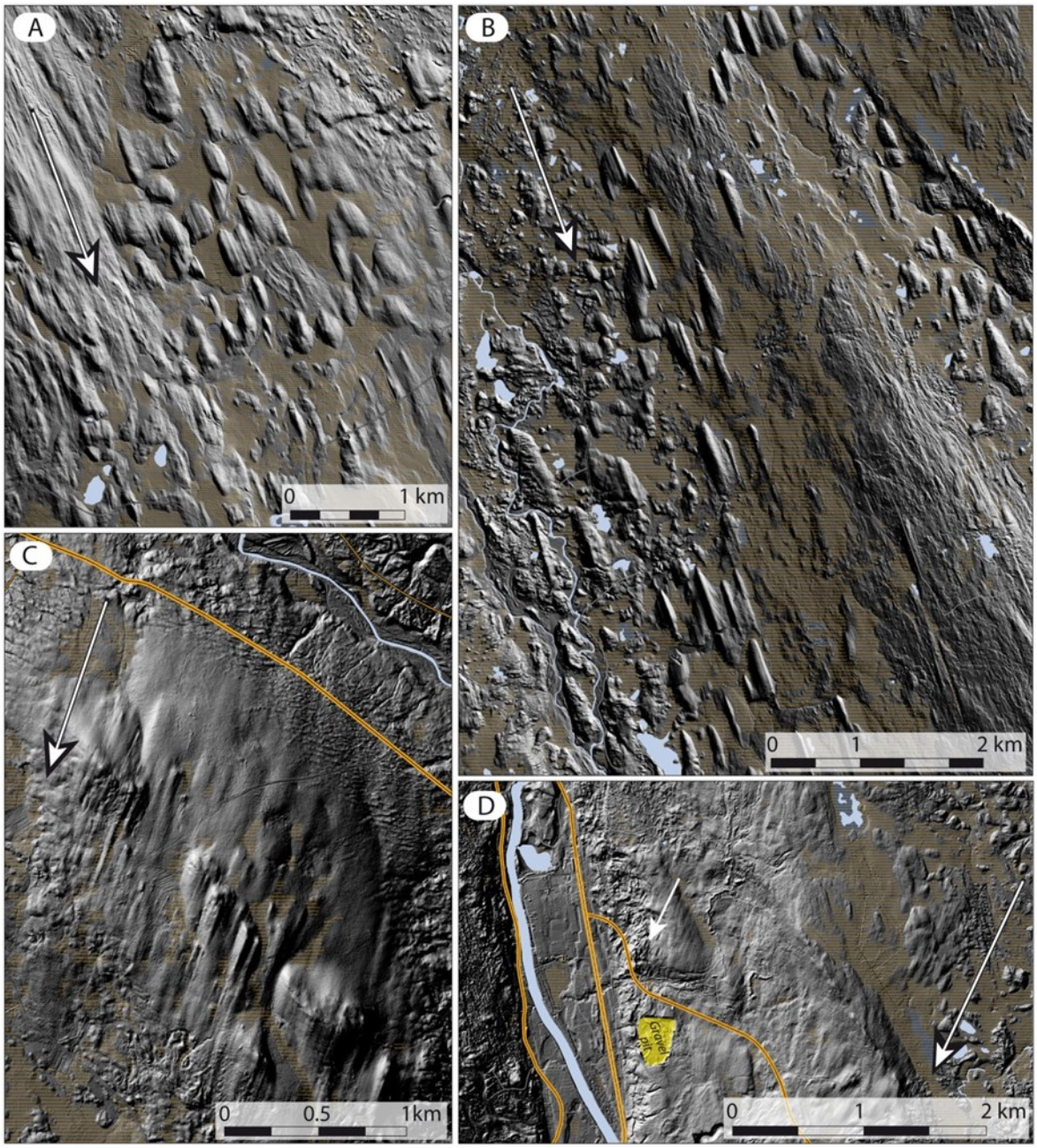

Fig. 6. (A) Streamlined terrain (drumlins and flutes), c. 15 km west of Fiskarheden (frame A in Fig. 5). Ice flow at streamlining is from 340˚ (NNW). (B) Streamlined terrain (drumlins and flutes), c. 25 km NNE of Fiskarheden (frame B in Fig. 5). Ice flow at streamlining is from 340˚ (NNW) (C) Streamlined terrain (drumlins and flutes), c. 8 km SW of Fiskarheden (frame C in Fig. 5). Ice flow at streamlining is from 18˚ (NNE). (D) Fluted surface north of Fiskarheden gravel pit (pit indicated by yellow area) and drumlins, c. 2.5 km to the east. Ice flow at streamlining is from 25˚ (NNE) (frame D in Fig. 5). Hill shade constructed from LiDAR scan data in the "New National Height Model" with a 0.2 m height and a 2*2 m width resolution (data provided by Lantmäteriverket, Sweden; ©Lantmäteriverket i212/927).

from the original ground surface, c. 150 m behind the main section wall (site 8, Fig. 4). Sections at sites 1-3 were cleaned by hand over lateral distances of c. 3 m and logged vertically at a scale of 1:20, using lithofacies codes according to the data chart in Table 1. The vertical and high nature of the main east to west trending section wall made it both difficult and hazardous to work due to its height, which was partly overhang and had falling pebbles. The upper parts were out of reach for logging but were well exposed due to the freshness of the actively quarried pit wall, and could be photo-documented from the pit floor. The lower c. 4 m of the section wall was cleaned by hand for a substantial part of its length and divided up in four section sites, 18 to 38 m long, and documented as section drawing on a photographic background. This was found much more suitable than vertical sediment logging, as revealed glaciotectonic structures are lateral in their extension rather than vertical. Sediments were classified to their facies states

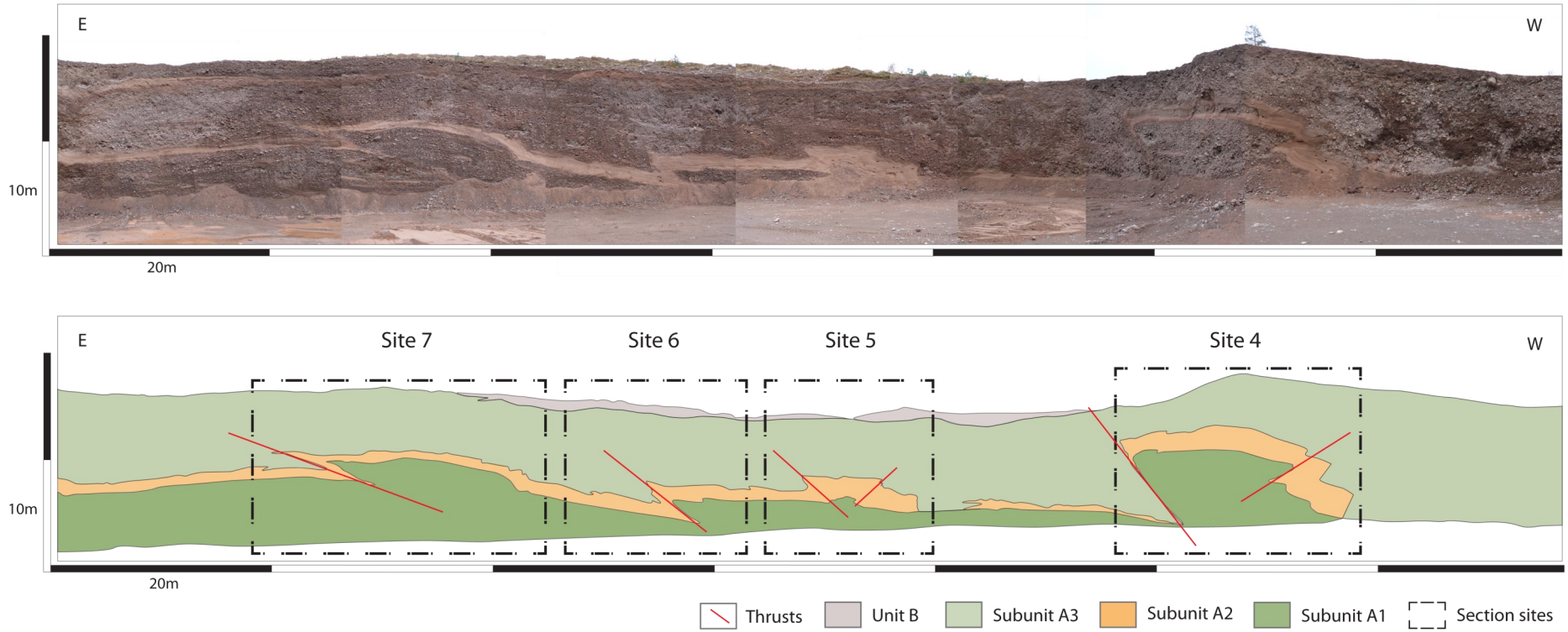

Fig. 7. Main section wall of Fiskarheden, trending E-W exposing sites 4, 5, 6 and 7 within each dashed squares. Subunit A2 is highlighted by an orange layer to have a quick overlook of the deformations features. Subunits A1 and A3 are respectively in pronounced green and paler green; Unit B is represented by a light purple to grey color.

according to Table 1, and glaciotectonic structures were described according to nomenclature in Aber *et al.* (1989) and Benn & Evans (2010) (Fig. 2). The lower part of the main section wall was mainly documented and internal features interpreted from pictures of the sections taken in-situ during field work. Several pictures were taken a couple of meters away from the cross section bottoms from the same location and were merged together in Photoshop. Pictures are in high resolution, allowing good analysis and correlation with the rest of the outcrop within the quarry pit.

The sections exposing the covering diamict at sites 8 and 9, and underlying glaciofluvial sediments, were cleaned by hand and documented by vertical logging at a scale of 1:20. Four clast fabric analyses in the covering diamict were done by excavating 50-30 cm wide horizontal shelves, with vertical sampling of pebbles less than 20 cm downwards from each shelf surface. Each fabric analysis comprises 25 pebbles, ranging between 2-10 cm for the longest axis (a-axis) and with an accepted ratio of the a/b-axis to ≥1, 5. All structural elements and orientation data (till fabric data, folds and thrusts in glaciofluvial sediments) were statistically treated according to the eigenvalue method of Mark (1973) and graphically simulated in StereoNet# (Allmendinger *et al*. 2013) to facilitate the overall interpretation.

A total of 12 samples were taken for OSL (Optically Stimulated Luminescence) dating from different parts of the exposed sections. Most of them (9) were taken by hammering PVC tubes into the central part of sand intrabeds between clast-supported cobble-gravel beds. However, we also sampled the top surface of some sand intrabeds (3 samples) during night conditions with red light. The purpose for this is to compare the OSL age for central positions of sand beds with the OSL age on top surfaces of bar lee-side sands, as it has been shown that sandur environments can be problematic for light exposure of the sand during transport in turbid water, and thus the potential of poor resetting of inherited quartz OSL signal (e.g. Möller *et al*. 2013). Our hypothesis is that sand bar surfaces were exposed to sun light at low stages, and thus with higher potential of being well bleached. The age determinations by OSL are beyond the scope of this thesis, and will be presented later.

Sweden's Ny Nationell Höjdmodell/new national height (NNH) model produced by the Swedish national mapping agency (Lantmäteriet; http://www.lantmateriet.se), uses Light Detecting and Ranging (LiDAR) (see technical description in Dowling *et al.* (2013)) and arrive to the end user at an average vertical accuracy of ~ 0.1 m and a pixel resolution of 2 m. The data is pre-processed to remove both wood cover and urban areas down to 'true' ground level. A hillshade model measuring c. 23x20 km was produced for illustrating the large-scale morphology of the area surrounding Fiskarheden (Fig. 5). Within this area some smaller areas were selected for demonstrating ice-flow patterns as revealed from streamlining (Fig. 6); the hill shade models were here constructed with illumination azimuths at 315° or 45° for best morphological display, all with an angle of illumination set to 20° and with a vertical exaggeration of 5. The hillshade models were produced with the software package ArcGIS10©.

5. Results

5.1. General geomorphology of the Fiskarheden area

The DEM scenes constructed from LiDAR height data demonstrate the overall NW-SE landscape trend, both on large-scale topography and overprinted Quaternary landforms , which is further enhanced in the up-scaled scenes (Fig. 6). Streamlined terrain with a strong NW-SE (340°) directional trend is very evident in Figs. 6A and B, showing up both as shorter drumlins and highly elongated flutes, most often occurring over slightly higher ground. In depressions are ribbed moraines, orientated perpendicular to the streamlined terrain and thus being part of the same glacial flow set. Streamlined terrain with this NE-SW trend have been suggested being of an older age than the last deglaciation since they do not reasonably fit into reconstructed ice-flow directions, nor at a post-maximum late Weichselian stage and neither to postulated ice-flow directions over the area at LGM with the ice divide of the Fennoscandian Ice Sheet (FIS) far east in the Baltic depression (Kleman 1990). Their exact age of formation is still unknown. Over smaller areas is streamlined terrain with drumlins and flutes indicating a close to 90° shift in trend, from 18° to 25°, i.e. from NNE to SSW (Figs. 6C and 6D). This trend is in accordance with what is suggested to have been the ice flow direction at the last deglaciation over the area (G. Lundqvist 1951; Kleman 1990) and in accordance with the approximately west to east-directed last deglacial recession lines drawn by Kleman (1990) over northern Dalarna.

5.2. General stratigraphy at the Fiskarheden site

The Fiskarheden gravel pit (Fig. 4) is situated on the eastern flank of the deeply incised Västerdalen River valley (Fig. 1), and within a larger area demarcated as glaciofluvial sediments beneath till in the mapping from SGU (Fig. 3). The till surface is at c. 412 m above sea level, and c. 62 m above the flood plain of Västerdalälven. The gravel pit was opened up in 1982 and is actively quarried southwards, up to now having an extension of c. 85 000 m^2. The quarry holds a 'U shape' planform (Fig. 4) with a main outcrop oriented east-west and facing north, exposing glaciofluvial deposits (unit A) topped by a diamict (unit B), the latter mostly removed along the section walls. According to the personnel operating the quarry the diamict has been varying in thickness between 0.5-4 meters. The main section (section 2, Figs. 4 and 7) is c.

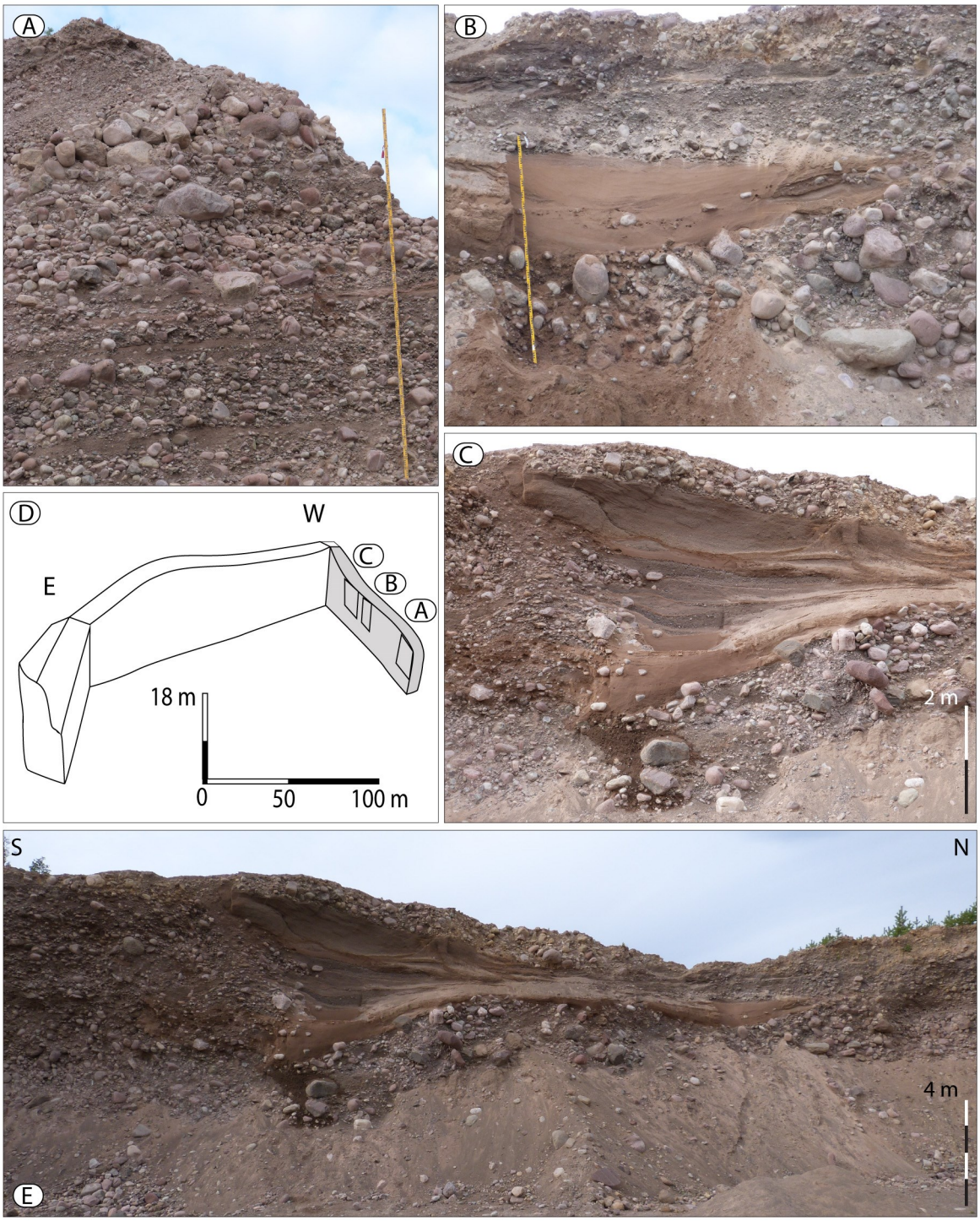

Fig. 8. (A) Photograph of site 1. (B) Photograph of site 2. (C) Photograph of site 3. (D) Positions of sections 1-3 along the east-facing pit wall (grey shaded). (E) Overview photograph of sites 2 and 3.

150 m long and between 13 m high, similar to the height in the western end of the quarried pit (section 1), and 19 m, as in the central part of section 2.

A striking feature in section 2 (Fig. 7) is a very continuous sand bed, varying in thickness between 0.8 and 5 meters. It is exposed all along the lower part of section 2, displaying large-scale glaciotectonics with Z -shaped forms. This sand unit is also present in the eastern section wall, facing west, but the glaciotectonics are here not that obvious due to the trend of the section in relation to the stress direction that caused them. As a stratigraphic marker, and also indicating a major shift in sedimentary energy over a large area at its emplacement compared to the sediments below and above it, it is designated subunit A2. The sediment successions above and below are very different in composition as compared to the subunit A2 sediments. They are made up of massive to vaguely stratified gravelly cobble to boulder beds, with minor constituents of stratified sands and gravels,

Table 1. Lithofacies codes (first-, second- and third-order code system) and their descriptions as used in this work (basic system according to Eyles *et al.,* 1983 and Möller)

Lithofacies code:	*Lithofacies type description: Grain size, grain support system, internal structures*
D(G/S/Si/C)	Diamicton, gravelly, sandy, silty or clayey. One or more grain-size code letters within brackets
D( )mm	Diamicton, matrix-supported, massive
D( )ms	Diamicton, matrix-supported, stratified
D( )mdg	Diamicton, matrix-supported, disorganized graded
D( )mm/ms(s)	Diamicton, …., sheared
D( )ms(a)	Diamicton, …., attenuated
D( )mm(ng)	Diamicton, matrix-supported, massive, normally graded
D( )mm(ig)	Diamicton, matrix-supported, massive, inversely graded
D( )mm (ing)	Diamicton, matrix-supported, massive, inverse to normally graded
B	Boulders
Co--	Cobbles, as below
Gmm	Gravel, matrix□supported, massive
Gcm	Gravel, clast□supported, massive
Gcm(ng); --(cng), --(mng)	Gravel, clast□supported,massive, normally graded; clast normal grading, matrix normal grading
Gcm(ig)	Gravel, clast□supported, massive, inversely graded
cS	Coarse sand
Sm	Sand, massive
Sm(ng)	Sand, massive, normally graded
Sm(ig)	Sand, inversely graded
Spp	Sand, planar parallel□laminated
Spc	Sand, planar cross□laminated
Stc	Sand, trough cross□laminated
Sr	Sand, ripple□laminated
Sl(def)	Sand, laminated, deformed
Sim	Silt, massive
Sil	Silt, laminated
Cl	Clay, laminated
Cm	Clay, massive

but also all of these showing glaciotectonic deformations, as will be described below. These sediments are designated subunits A1 and A3, respectively. Sediments exposed along section 2 are documented in consecutive sections, numbered as section sites 4-7 (Fig. 7)

Three test pits in front of the main section wall were dug to depths between 4 m and 7 m (Fig. 4). A seemingly new sand bed similar to subunit A2 and c. 4 m thick forms an anticlinal structure, reaching close to the pit floor in the central trench, but covered by the coarse-grained unit A1 in the other trenches. This sand unit is referred to as subunit A0. However, it could not be investigated due to the unstable test pit walls, the pits thus too dangerous to enter.

The subunit A2 sand descends towards the west and is not exposed in section 1, but is probably present behind the basal scree cone of this section, which is a left-over ridge from previous quarrying. The sediments exposed here correspond to subunit A3 in section 2 and are logged in more detail as they were more easily reachable (section sites 1-3, Figs. 8 and 7). No glaciotectonic deformations are seemingly displayed in this section wall. This is probably due to its trend, being perpendicular to the deformation direction displayed in section 2 (see below). Below is a detailed sedimentary description of the sediments at the documented sites along the section walls.

5.3. Sedimentology of section 1

5.3.1. Descriptions

The sediments exposed along section 1 reveal no obvious deformation structures, which most probably is due to the section's orientation with respect to the tectonical stress direction (i.e. approximately perpendicular to the trend of section 2, revealing large-scale tectonics). The logged sediments thus expose original bedding even if they possibly are within a larger tectonically displaced sediment stack. As such, the logged sequences thus give a more secure framework for sedimentological interpretation.

Site 1. - The section wall at the logged site (Fig. 8D) is 10 m high (Figs. 8A), but only the uppermost 5.75 m could be logged as the lower part was covered by scree material (Fig. 8A). It is mainly composed of stacked sets of clast-supported boulders and cobbles, the beds 80 cm thick, interbedded with thinner beds of laminated gravelly sand and sand. The sediment succession represents subunit A3's facies. The five logged cobble/boulders beds have maximum boulders diameter of 25 cm, and sometimes display open frameworks, sometimes matrix infill of sand and fine gravel. Cobble and boulder roundness varies from well -rounded to angular. The interbedding sand beds often carry intrabedded thin gravel beds or just gravel stringers.

Site 2. - The section wall at the logged site (Fig. 8D) is 6 m high, but only the uppermost 3.3 m could be logged as the lower part was covered with scree material (Figs. 8B, 8E and 9B). The sequence consists of two thick beds of clast-supported cobbles and boulders (subunit A3), with maximum boulder sizes of 40 cm and with frame-work infill of sand and fine gravel. Cobble and boulder roundness varies from well -rounded to angular. The upper bed also host small laminated sand intrabeds. In between is a complex set of interbedded planar parallel-laminated and cross-laminated fine to coarse sand and gravels, and also a cobble/gravel stringer as a continuation from clast-supported coarse beds (subunit A3) in lateral direction (Fig. 8E). The fine-grained interbeds thin to the right and fade out in the subunit A3 surroundings.

Site 3. -- The section wall at the logged site

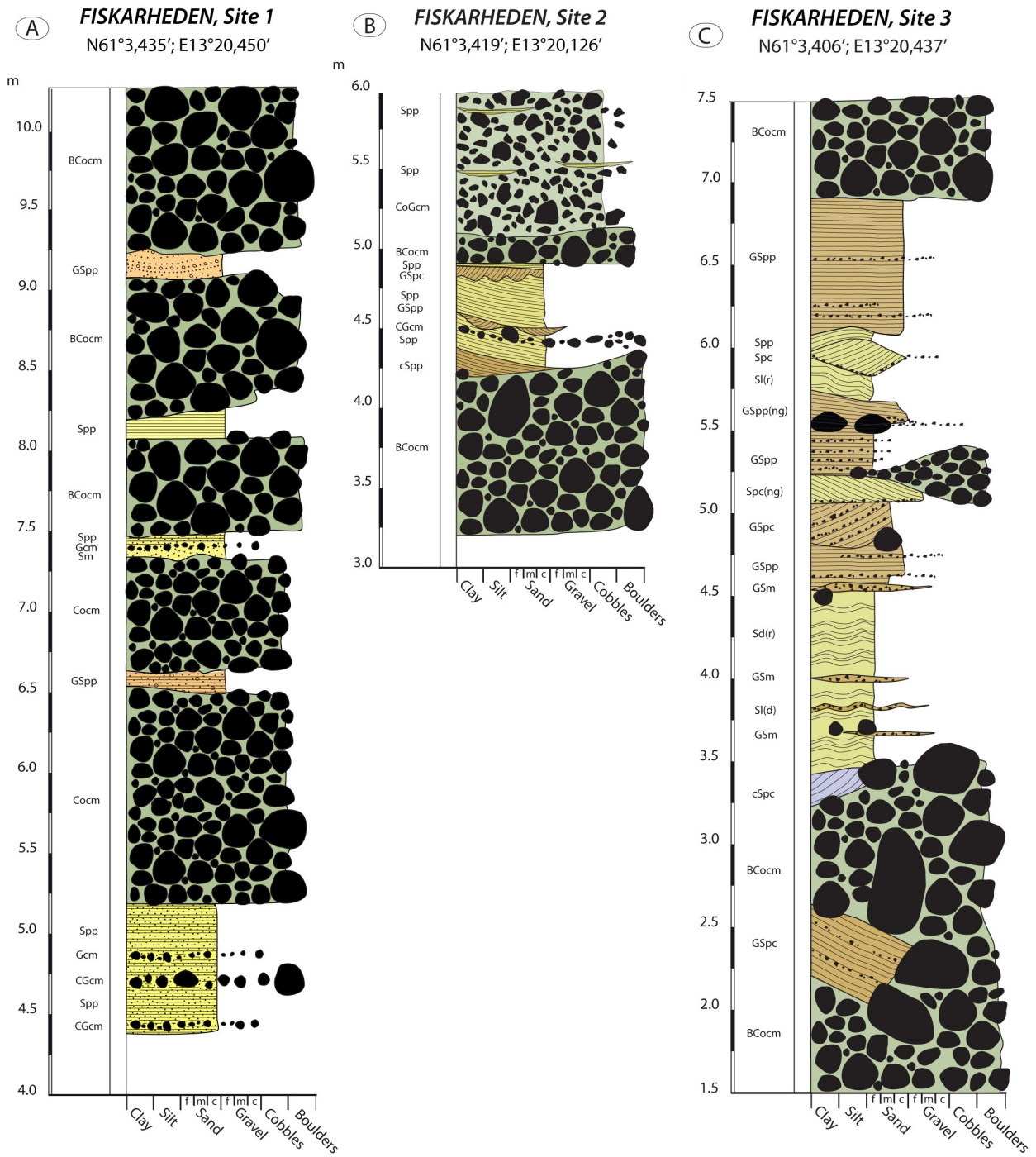

Fig. 9. Sedimentary logs of sites 1–3 (locations shown in Fig. 4). Lithofacies codes according to Table 1. Note: the colors used in the descriptive logs are the same used in the illustration made

(Fig. 8D) is 6 m high (Figs. 8C, 8E and 9C). At the base and top are clast-supported cobble to boulder sediments (subunit A3), the lower one with maximum sizes of c. 60-70 cm and the upper one with maximum clast sizes at c. 50 cm. Cobble and pebble roundness varies from well-rounded to angular. Parts of the sediments show open frameworks, while other have sand and gravel matrix infill. In between is a complex sequence of finer-grained sediments (3.75 m thick) that thins out in lateral direction towards site 2 (Fig. 8E), and is also laterally split up by an interfingering clast-supported cobble bed, as indicated at c. 5.2 m in the log. This more fine-grained sequence is composed of gravelly sand being planar parallel-laminated and planar cross-bedded, interbedded with intercalated sets of ripple-laminated sand and thin beds of massive gravelly sand. Out-sized (10-35 cm) single to lined-up clasts occur within beds or at bed contacts, and often show scour pools around them.

5.3.2. Sedimentological interpretation, sites 1, 2 and 3 (section 1)

The very coarse, massive and clast-supported beds in section 1, as well as those in sections 2 and 3, are interpreted as remnants of longitudinal bars, formed from deposition clast by clast from a bed-load

transport with vertical accretion in a braided river environment (Miall 1977). Clast roundness indicates an insufficient transport length for all angular and sub-angular clasts to be changed in their morphology, consistent with deposition in an ice-proximal position. Open frameworks suggest by-pass of the more fine-grained load, whereas sand to gravel matrix between clasts suggests late-stage infill during waning flow stages. Interbedded thinner sand beds were most probably deposited at the same time as the coarse bars, but in lower-energy environments distal to bar accretion as at the lee of bars or bar edges (Miall 1977). As the bar is aggrading and slightly prograding, the finer-grained sediment will show interfingering with the surrounding bar deposits (Miall 1977; Zielinski & van Loon 2003). In summary, the section 1 sediment sequence is very similar to the *Scott type* facies association described by Miall (1977) forming in very proximal sandur settings (Zielinski & van Loon 2003), with a high sediment supply relative to water discharge (Fig. 10).

The much thicker sand intrabeds together with gravel and cobble stringers in section 3 suggest deposition in deeper, between-bar, channels that were not evacuated of their sediment infill during a later high-flow stage and thus preserved as younger coarse-grained bar sediments migrated over the channel fillings. The planar beds with gravel stringers suggest flow in upper-flow regime, as do scour pools around out-sized clasts, and trough- and planar cross-bedded unit suggest 2D and 3D dune migration in these channels (Fig. 10), while ripple-laminated sand suggest bed-load deposition during ripple migration at lower-energy stages. The sediment succession as revealed in sections 2 and 3 are still regarded to belong to a proximal sandur environment, but possibly representing deposition in side/secondary channels with lower flow discharges (e.g. Zielinski & van Loon 2003).

5.3.3. Age determination on the sandur sediment in section 1

Three samples for OSL dating were taken in 2012 in sand intrabeds close to section 1 (Fig. 8A) of this study. The dating results (personal communication, Helena Alexanderson and Per Möller) show high doses (>300 Gy) that are close to saturation in measured quartz grains, and thus actually beyond the limit for giving reliable OSL ages for quarts grains (Möller *et al.* 2013). Nevertheless, calculated ages for these samples are thus very high, 215 ± 13, 269 ± 17 and 271 ± 18 ka, respectively. If these ages are on well reset sediments, and thus representing true ages though a bit beyond the technical limit for quartz of the method, these suggest a pre-Saalian age of the sandur sediment. However, ice-proximally deposited sandur sediments can be notoriously difficult to get accurate ages on due to poor bleaching in turbid melt-water; Möller *et al*. (2013) show from a nearby site at Idre that proximal sandur sediments gave much older ages than underlying MIS 3-aged glaciolacustrine sediment (9 samples with ages between 41 and 54 ka, with a mean age of c. 45 ± 2 ka), while overlying proximal sandur sediment came out with OSL ages between 130 and 180 ka (mean age c. 156 ± 13; n=4). It is thus strongly suspected that the three retrieved OSL ages from Fiskarheden should be regarded as maximum age for sediment emplacement; true age could be anything from pre/post-Saalian to any of the ice advance/retreat phases within the Weichselian stadial/interstadial/ stadial transitions over the area as, e.g. as depicted in Kleman *et al.* (1992). Future treatment of taken OSL samples (in total 13 samples) will hopefully shed more light on the chronologic issue, as it is planned measurements also on feldspar grains and on single quarts grains (personal communication, Helena Alexanderson and Per Möller). This, however, is beyond the scope of this thesis.

5.4. Stratigraphic and sedimentologic architecture of section 2

5.4.1. Generalized sedimentologic subunit (A1 - A3) descriptions

As described in section 5.2 above, the sediments displayed along the main pit wall (section 2) are deformed, the glaciotectonic structures partly erasing primary sedimentary structures. In spite of this, each documented site along the section show the same sediment architecture with their sedimentary subunits laterally traceable. The sorted sediment has thus been assigned to one sediment unit and divided into 3 subunits, A1, A2 and A3. Unit A is covered by a diamict (unit B) along the entire section, but which is mostly removed due to the quarrying activity. The unit B diamict is better preserved at sites 8 and 9 outside of section 2 (Fig. 4), from where it is described (see 5.6). As mentioned in the introduction (see 5.2) there is a lower sand unit designated A0 that resembles subunit A2, hidden beneath the present floor of the quarry. Below is a summary account of the primary sediment facies (facies associations) hosted within the stratigraphic subunits A1, A2 and A3, as shown in section 2 at sites 4-7 (Figs. 7 and 10). Tectonic overprints will be described separately for each section later on (see 5.5).

Subunit A1. - Dominating facies is clast-supported, massive to vaguely stratified gravelly cobble to boulder beds, some beds with open framework and others with a sandy gravelly matrix infill. Maximum clast sizes are around 80-100 cm, and the most common clast size is 15-25 cm. Interbedded with the coarse beds are gravelly sand and sand, the beds laterally traceable along the projection of section 2 between 4-45 m. These beds vary from being massive to showing planar parallel laminations, and also stacked sets of trough cross-laminated gravelly sand occur, individual sets being up to 40 cm thick and 2.4 m wide. Exposed subunit A1 sediment vary in thickness along the section between 1 and 9 m, and

have a sharp contact towards the subunit A2 sand, though the original, presumable horizontal (Fig. 10) contact is heavily deformed due to the overprinted large-scale tectonics in section 2 (Fig. 7). The basal contact of subunit A1 is not exposed, but it is terminated below the pit floor at 0.5-3.5 m depth towards a lower sand unit (subunit A0), as revealed from three test trenches dug in front of the pit wall.

Subunit A2. - The architecture of the subunit A2 sand is zig-zag formed due to the glaciotectonic overprint. It can, however, be followed continuously along section 2, in thicknesses varying from 80 cm (east part of site 7) to 4-5 m (sites 4, 5, 6) (Fig. 7). Though thus deformed to their position in sections 2, the contacts with subunits A1 and A3 are sharp. However, the internal primary beddings are well preserved. The facies association is dominantly composed of laminated light orange medium sand, but also laminated dark coarse sand and gravelly sand beds. A minor facies association constituent is a massive and thin (maximum 10 cm) clay intrabed, present at sites 5 and 6 (Figs. 13 and 14). Planar laminations are omnipresent as well as some planar and through cross-beddings. There is a frequent occurrence of sediment intraclasts, 10-nb 15 cm in diameter, blocky in appearance and to enclosing sand. The intraclasts show well preserved internal laminations when sandy and are usually massive when they are silty clay to clay clasts.

Subunit A3. - This unit has similar composition and characteristics as subunit A1. The thickness varies between 3 to 10 m and spread over sections 1 and 2, the thickness differences due to the tectonic displacement of the original position of the sediment. The basal contact with subunit A2 is sharp and well defined, though deformed to its position. As for subunit A1, subunit A3 mainly consists of clast-supported, massive to vaguely stratified gravelly cobble to boulder beds, some beds with open framework and others with a sandy gravelly matrix infill. Maximum clast sizes are around 80-100 cm and most common clast size is 15-25 cm. This coarse facies is interbedded with beds of gravelly sand and sand, up to 50 cm thick and 3 m wide for the smallest and one large sand strata spreading over the eastern part of site 7, but thinning toward the west. This bed can be followed for 50 m to the east and is around 2.5 m thick. These beds show planar lamination, cross bedding, or are simply massive.

5.4.2. Sedimentologic interpretation of subunits A1- A3, section 2

The dominating clast-supported boulder to cobble beds and their interbedded sand and gravelly sand beds of subunits A1 and A3 along section 2 are similar to those exposed along section 1 and are thus interpreted similar. The very coarse, massive and clast-supported beds are thus interpreted as remnants of longitudinal bars, formed from deposition clast by clast from a bed-load transport with vertical accretion in a braided river

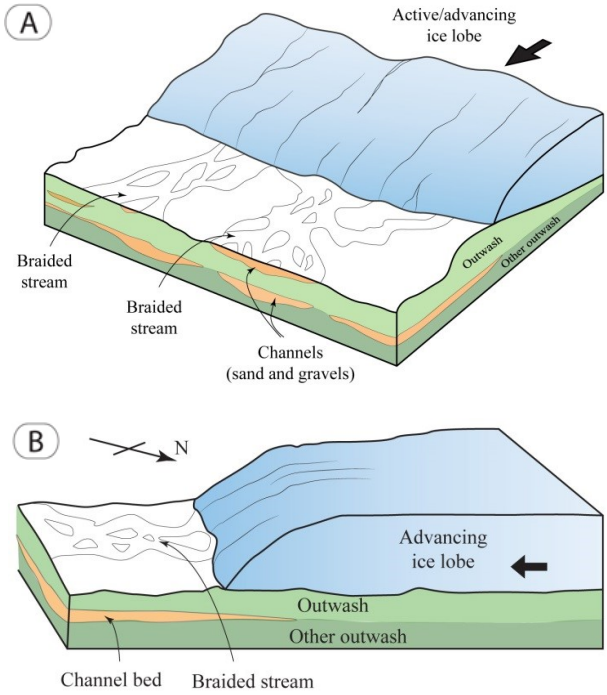

Fig. 10. (A) 3D illustration of the palaeoenvironment at deposition the of Fiskarheden sandur succession. Sediments were deposited in a proglacial proximal position as suggested by its resemblance to Trollheim or Scott sandur succession types (subunits A1 and A3). Internal architectures also indicate some dramatic changes in depositional environments on the braid-plain system as suggested from the transfers between subunits A0/A1, A1/A2 and A2/A3 (see text for further explanations) (B) 3D lateral view of the Fiskarheden sandur succession prior to deformation.

environment (Miall 1977). The finer-grained interbeds are interpreted to represent preserved late-stage infills in secondary braid channels or sediment deposited in lower-energy environments distal to bar accretion as at the lee of bars or bar edges (Miall 1977). With continuing bar aggradation and progradation, the finer-grained sediment would interfingering with the surrounding coarse-grained bar deposits (Miall 1977; Zielinski & van Loon 2003). Subunits A1 and A3 sediments along section 2 thus suggest deposition in a very proximal braid-plain setting (Zielinski & van Loon 2003) with similar facies associations as depicted for the *Scott type* facies model by Miall (1977), and resembling architectural elements that can be recognized in many contemporary proglacial systems (Benn & Evans 2010) (Fig. 10).

Subunit A2 marks an abrupt and drastic shift in depositional environment from the gradual vertical aggradation of proximal-type sandur deposition of subunit A1. The same abrupt back-wards shift to 'normal' proximal-type sandur deposition happens at its upper contact with subunit A3. Finer-grained sediments within subunit A1 and A3 have, as described above, very limited vertical and lateral extensions and represent minor channel infills or bar-lateral/bar lee-side deposition. The fine-grained sediment succession of subunit A2 comes with a very

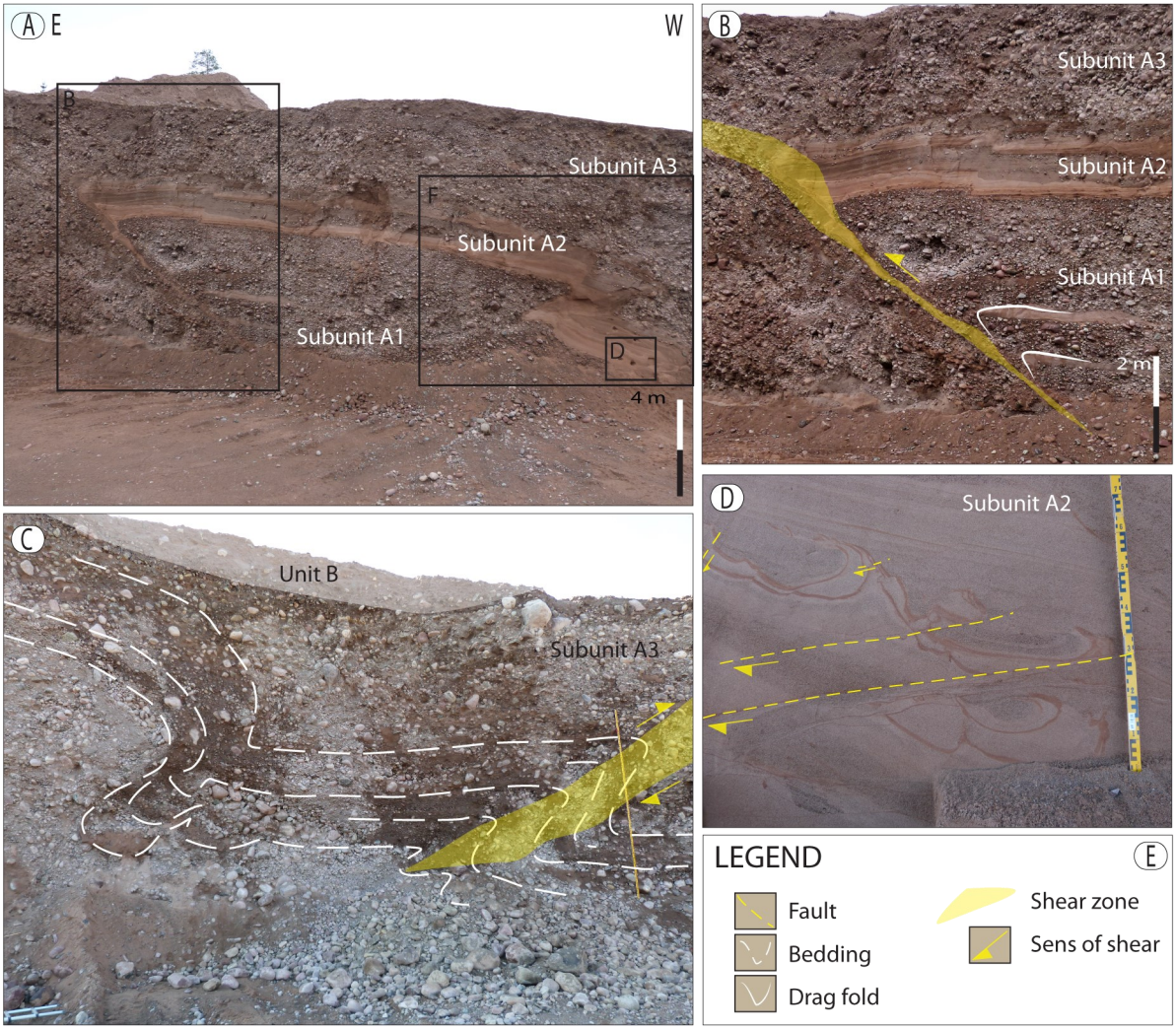

Fig. 11. Sediments and structures at site 4. (A) Photograph overview covering area A in subfigure (G); Black frames indicate positions for following subfigures. (B) Close up of the thrust system in the left-hand side of the section, marked by the yellow zone; note the normal drag folds (Fig. 1) above the thrust, indicated by white lines. (C) Western part of the section (area C in subfigure G) with disturbed original bedding of subunit A3 indicated by dashed white lines; fan and overturn folds. (D) Close up of the faulted convolute structures, the red silty sand lamina cut by low-angle reverse faults. (E) Legend for the preceding drawings. (F) Photograph of the lower right-hand side of section 4. (G) Positions of subfigures (A) and (C) along the main section wall. (H) Legend for the section drawing in (I). (I) Section drawing of the lower right-hand side of section 4, including structural data.

distinct contact to subunits A1 and A3 and covers the entire depositional surface of subunit A1 as exposed in the gravel pit (i.e. hundreds of meters in all directions). It can thus not represent a kind of low-stage preserved channel fill, but is suggested to mark a major sedimentological event, possibly a catastrophic flood event such as a glacial lake outburst floods (GLOF; Benn & Evans (2010)) or jökulhlaups, as described among others by Maizels (1993a, 1993b, 1997) and Russell & Marren (1999). The subunit A2 sediment succession thus suggests a sudden 'drowning' of the preexisting braidplain with deep water invading the overall braidplain, possibly with some erosion but also infill of existing channels. The stream flux must have carried a high sediment load, most of it falling out of suspension with a short phase of traction, resulting predominantly in the recorded planar lamination, possibly in upper flow regime. At a few places deposition was from sediment traction only, such as migrating 2D and 3D dunes, as suggested by cross-bedded sediments at sites 5 and 6 (Figs. 13 and 14). The sediment intraclasts, especially common at site 4 (Fig. 11J), show well-preserved internal laminations but do not match the internal laminations of subunit A2, and suggest that these must represent frozen sediment blocks, eroded upstream and transported in a frozen state downstream, where they were embedded in subunit A2 sediments (Fig. 11I).

The sharp contact to above-lying unit A3 sediment, suggests as abrupt termination as initiation of this outburst flow event, changing the depositional environment back to proximal-type gradual sandur aggradation once more (subunit A3).This suggested outburst flow event might not be a single such over the entire build-up period of the Fiskarheden deposit; the sandy subunit A0, observed in the previously

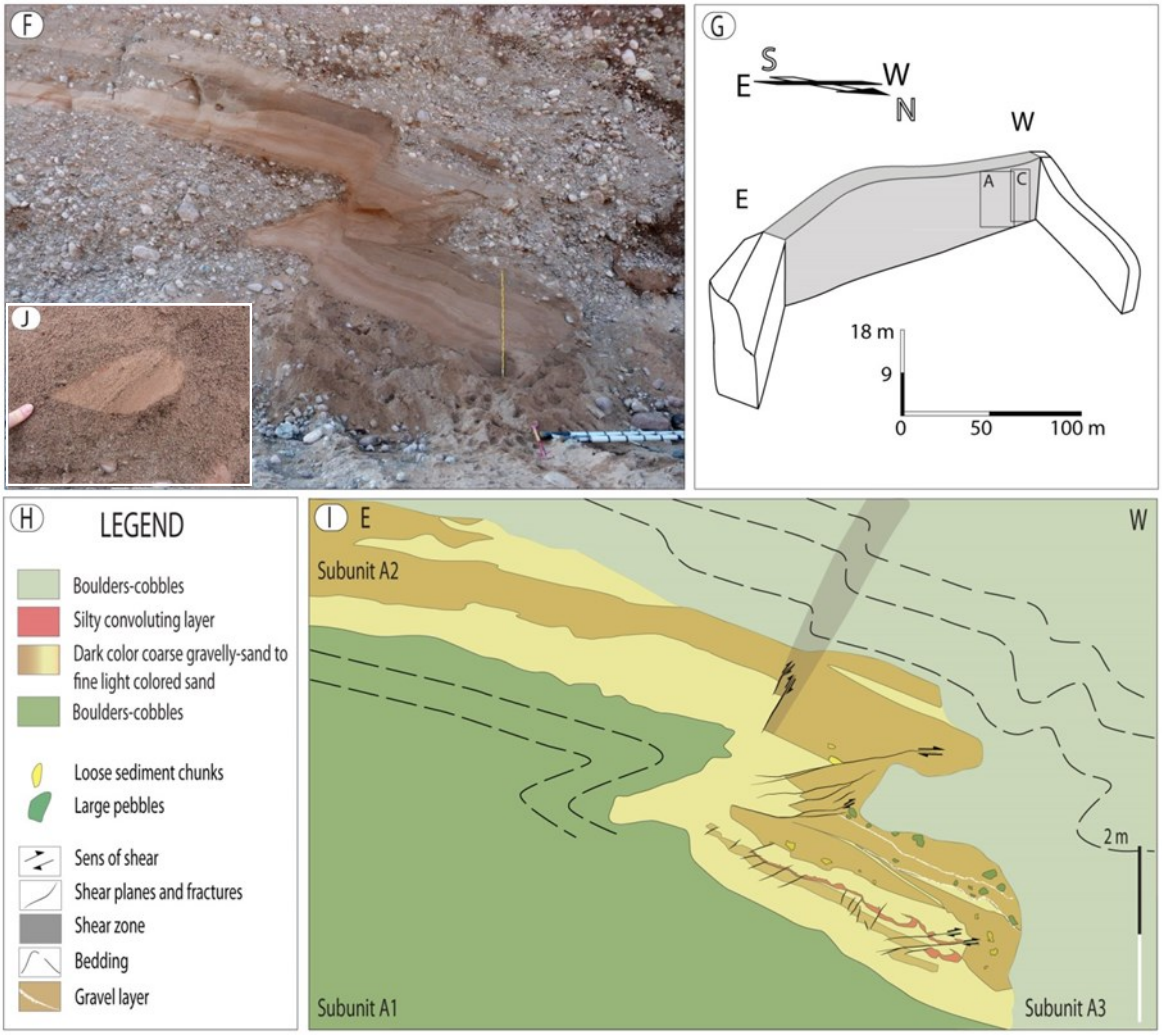

Fig. 11. continuation

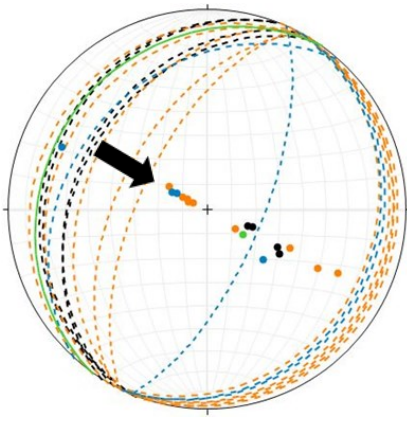

Site 4: Faults
S_1=0.71
V_1=118.4°/45°
n = 4

Site 5: Faults
S_1=0.92
V_1=208°/25°
n = 10

Site 6: Faults
S_1=0.85
V_1=212°/43°
n = 4

Site 7: Fault
S_1=1
V_1=215°/18°
n = 1

Fig. 12. Sites 4 (blue), 5 (black), 6 (orange) and 7 (green) Stereonet plotted data from shear planes of each section site. Calculated normalized eigenvalue (S_1) and strongest eigenvector (V_1) are shown, as well as interpreted ice flow direction (black arrow).

described three test pits (Fig. 4), might reflect a similar event.

5.5. Site-specific sedimentology and glacial tectonics along, section 2

As described above, the sediments displayed along the main pit wall (section 2; Fig. 7) show intense tectonic deformation that needed close examination for its interpretation. Stratigraphic subunits A1, A2 and A3 will be described below for their site-specific sedimentology at each site individually, followed by structural description of the glaciotectonics.

5.5.1. Site 4

Sedimentary composition. - The section site is 25 m wide and 13 m high and exposes highly disturbed sediments (Fig. 11A). The lower 5 meters were studied in detail (Figs. 11F and 11I) after hand excavation of 1 m of scree material, whereas the topmost parts could not be reached due to an overhanging cobble wall. However, it was photographed and studied from a distance. The section contains subunit A2 sand in its middle part, with sharp contacts to subunits A1 and A3 at its bottom and top. Subunit A2 is 3.5 m thick in the central part of the section site and 2 m elsewhere. It

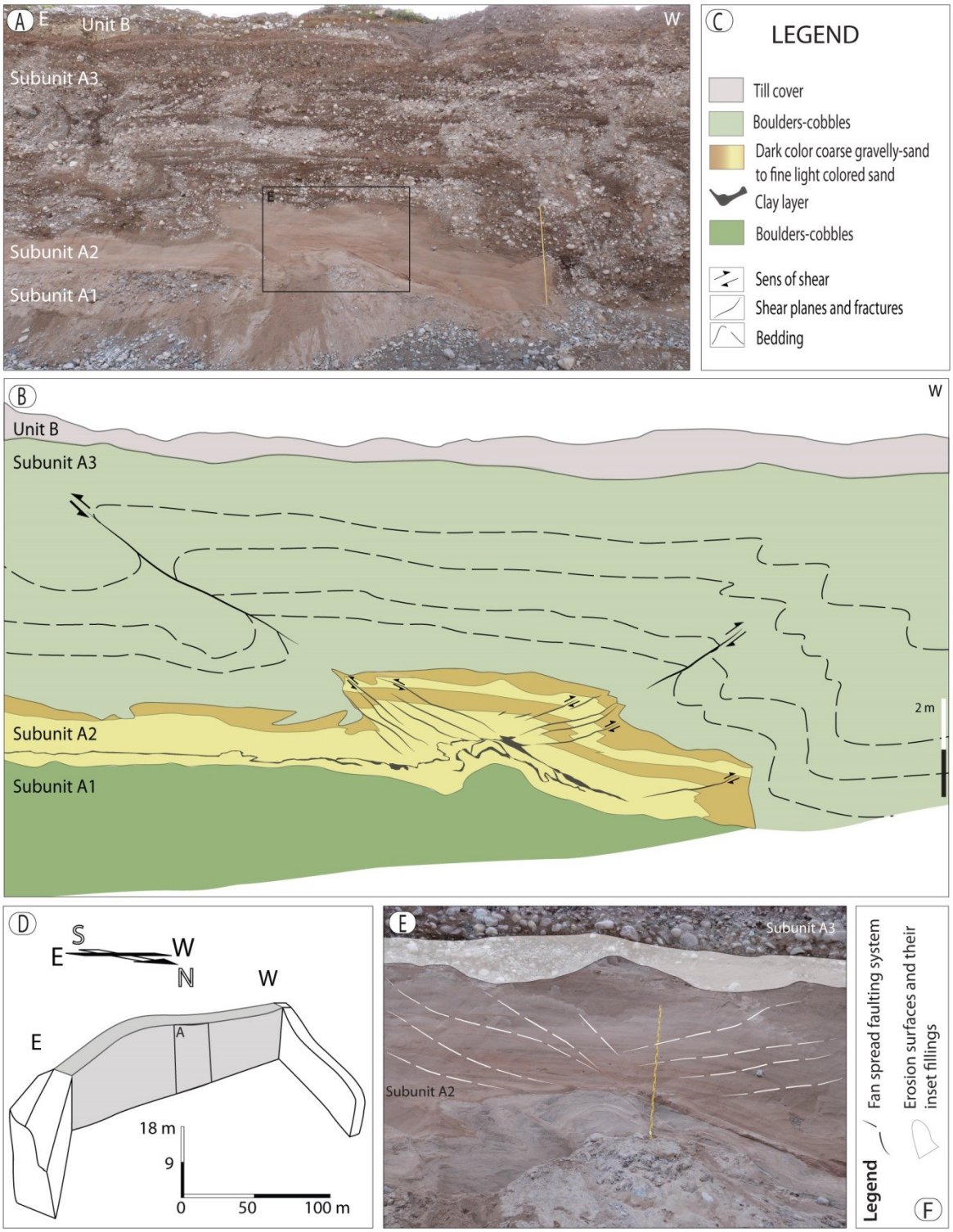

Fig. 13. Sediments and structures at site 5. (A) Photograph overview. (B) Section drawing of the entire site, including structural data. (C) Legend for the diagram. (D) Position of section along the main section wall (gray shade) and covered area of photograph. (E) Close up on the middle part of subunit A2; a fan-spread faulting system. Marked is the upper part of erosion surfaces below the contact with subunit A3. (F) Legend for figure (E).

can be split up into a lower part with a lighter fine to medium sand and an upper part with darker coarse sand and gravelly sand (Fig.11I). The internal features are laterally traceable along the entire section site (Fig. 11A). The coarser sand often contains floating pebbles and intraclasts of laminated sediment with blocky appearances (Fig. 11I). Convolute bedding, interpreted as water escape features occur frequently in the western lower part of the section (Fig. 11D), and are highlighted by red sand markers. The top-most part of the site within subunit A2 shows undeformed trough cross-bedding structures (Fig. 11A). The boulder-cobble, top and bottom members (subunits A1 and A3) demonstrate well-defined internal bedding within the

coarse boulder-cobble-gravel sediments.

Tectonic architecture and structural description. - The overall tectonic appearance of site 4 show fault-propagation folding resulting in two Z-forms in subunit A2, facing each other (Figs. 7 and 10A). The stiff Z shape in the lower right-hand part of the section (Figs. 11F and I) contains multiple small and medium scale deformations, mainly brittle reverse -type fractures and faults. The fault planes are striking between 19-35°N with dips (18-68°) towards the east (Fig. 12). These faults are high-lighted when, e.g., cutting through laminated intraclasts (Fig. 11D). Sub-vertical faults, striking 23-40°N can also be observed, usually well-defined but shorter in length and almost only occurring within the coarser sand (Fig. 11I). The opposing Z shape to the east of the section (Fig. 11A) is sheared down into a thrust-fault breccia (Fig. 11B) marked by a high-strain, 10 m high reverse thrust zone, striking 241° (SW-NE) and dipping 46° towards NW (Fig. 12).

Subunit A2 can only be followed for 1-2 m down into the thrust system. Laminated intraclasts are seen to be broken down and dragged into the cataclastic system, continuing into a cataclastic (or mylonitic) thrust fault breccia (Fig. 11B) that almost ends the continuity of the subunit A2 sand until it reaches the bottom sand layer, assumed to be the lateral match of the sand at the top of the Z form. Along the thrust plane, smaller sand layers within subunits A1 and A3 show convex drag folds (normal drags) (Fig. 2) when in contact with the shear zone (Fig. 11B).

Subunits A1 and A3 are also showing deformations, but of ductile to ductile-brittle types. Subunits A1 and A3 contain major overturns of original sedimentary bedding, including recumbent as well as fan folds (Fig. 11C). The fold hinges in the subunit 3 coarse sediments have matching fold axes with the internal subunit A2 faulting axes system. Some of the folds are close to the brittle system and demonstrate almost a growing tip of an eventual thrust fault (Fig. 2).

The overall structure revealed by the deformations of subunits A2 and A3 is a sort of stretched axial surface to one side and an opposite compacted axial surface box fold (Fig. 2). It almost has similar features as a 'one side' pop-up structure (Fig. 2), to the left almost with kinking to its top corners.

5.5.2. Site 5

Sedimentary composition. - The part of the section wall designated site 5 is 18 m long and 17 m high (Figs. 7 and 13D). The sand bed is laterally traceable from section 4, and is here 2 m thick and stands out texturally from overlying subunit A3. The boulder-cobble bottom member is poorly exposed in this section. The lower part of the sand bed is laterally traceable until site 6 (Fig. 7). It consists in its lowermost part of light colored sand, the original bedding enhanced by darker layers. Above these is a clay bed that is ~2-30 cm thick, and lined with imbricated large (~10 cm) cobbles. The clay bed thickens considerably towards the center of the section (20 cm) where the main deformations are located (Fig. 13B). It also splits up into a very deformed layer, almost like capillaries, intrabedded with laminated coarse sand in the center part (Figs. 13B and E). The upper part of the sand bed consists of clear erosion surfaces (Fig. 13E). The surrounding boulder-cobble members show massive cobble-gravel beds with both open frame-works. Those with gravelly matrix infills are interbedded with short/discontinuous sand beds.

Tectonic architecture and structural description. - The deformation within subunit A2 displays a brittle-type fan-shaped spread faulting (Figs. 13A and B), forming a pop-up structure (Fig. 2). The reverse faults on the left-hand side strike between 199-225° with dips 21-35° towards the NW, while the faults on the right-hand side strike 10-22° with dips of 9-12° towards the E (Fig. 12). The cobble-pebble beds of subunit A3 on top show similar deformational features as described from section 4. Ductile deformations are recognized as propagations from those in subunit A2, with fault lines and associated drag folds correlating with the strike and dip of the faults located below in subunit A2 (Fig. 13B). To the east, also in subunit A3, chevron folds turning into normal drag tales (Fig. 2) within a thrust system can be seen, as well as another fan fold (Fig. 2) squeezed in between the drag folds and the bedding (Fig. 13B). The system turns into a brittle-ductile deformation there. The overall shape of the section wall is almost a standard pop-up structure.

5.5.3. Site 6

Sedimentary composition. - The part of the section wall designated site 6 is a lateral continuation of site 5 (Fig. 7); the section site is 18 m long and is the highest along the main section, 19 m (Fig. 14C). Subunit A2 shows alternations of light medium sand and darker sandy gravel layers and this internal bedding highlight the deformations of the subunit. The topmost part of the sand bed has a sharp erosional surface with subunit A3 (Fig. 14D), as is the case at site 5. The top and bottom boulder-cobble members (subunits A1 and A3) show massive cobble-gravel beds with both open frame-works and those with gravelly matrix infills, interbedded with short/discontinuous sand beds.

Tectonic architecture and structural description. - The internal deformation within subunit A2 is characterized by brittle-type fractures and reverse faults. One major inverse fracture-fault can be followed from the left edge top of subunit A2 downwards to the bottom right corner of the unit (Figs. 14B and D). It strikes N27° with a dip of 17° towards NW when a fault and dips 52° towards NW when more of a fracture (Fig. 12). Other deformations here are within the same range as the other sections described, with faults striking between 27-69° with

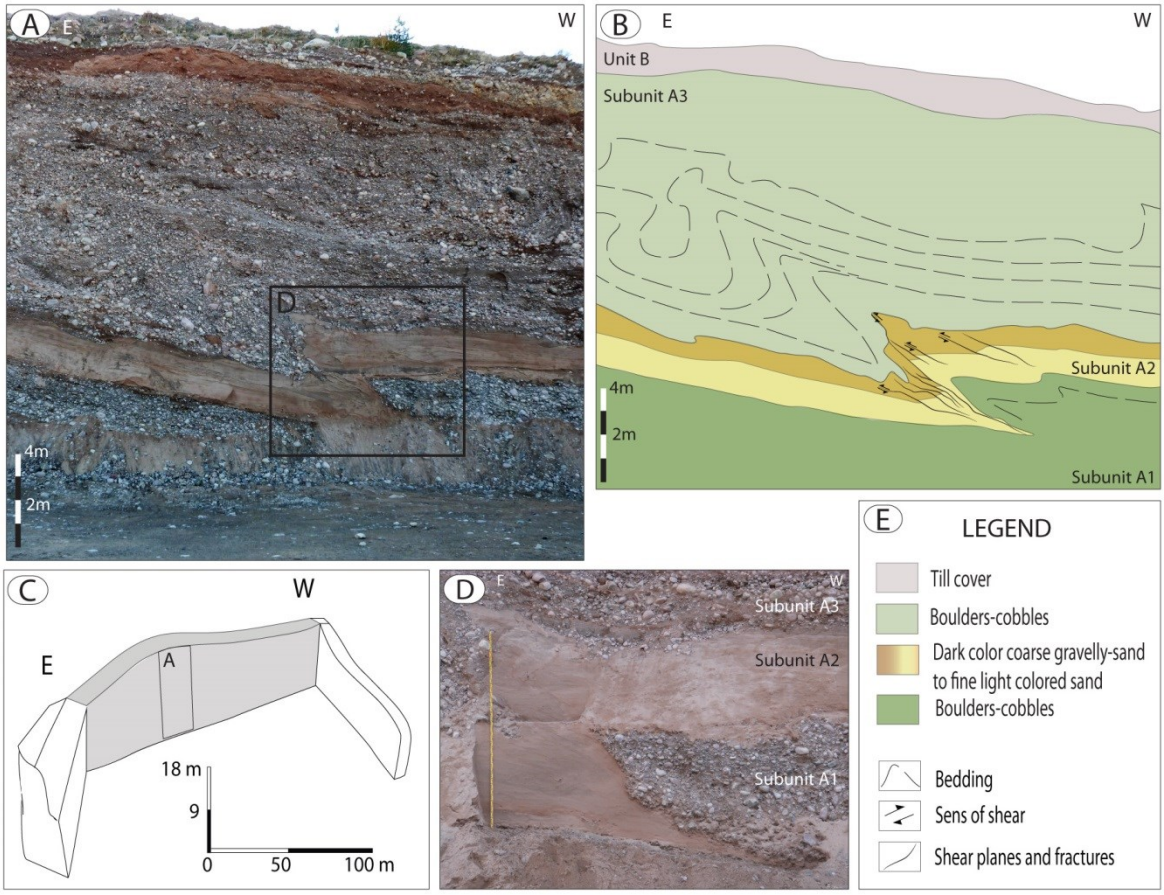

Fig. 14. Sediments and structures at site 6. (A) Photograph overview; black frame shows position of figure (D). (B) Section drawing, including structural data. (C) Position of section along the main section wall (gray shade) and covered area of photograph (A). (D) Close up of the central part of then section with the 'reverse Z shape' structure of subunit A2.In the western part of the section are fan and overturn folds of the original bedding indicated by dashed lines. (E) Legend for the diagram in figure (B).

dips 17-23° towards NW (Fig. 12). Minor reverse shear planes occur in the top part and reveal an opposite dip; these strike between 159-163° and dip 29 -59° towards ESE. As a continuation of the thrust structures within subunit A2 are chevron folds (Fig. 1) within the cobble-pebble cover of subunit A3 (Fig. 14B), thus matching the top left part of subunit A2 and following the strike and dip directions of the fracture there (N27° with a dip of 52° towards NW; Fig. 12), as well as a fan fold (Fig. 2). Some small scale overturned chevron-like folds in subunit A1 also matches the subunit A2 deformations.

5.5.4. Site 7

Sedimentary composition. - The part of the main section wall designated site 7 (Fig. 7) is 19 m high and 52 m wide (Fig. 15) and shows clear lateral sediment continuity from site 6. Detailed observations could not be carried out due to safety concerns, but pictures were taken and allow a good basis for description. Subunit A2 has a sharp contact with subunit A1 and subunit A1 can be 1 to 8 m thick there. To the right (west) side of the site, the sand bed is 2.5 m thick and thins laterally to the left (east) to 1 m in thickness in the center and then thicken up to 2.5 m. The sand bed is similar to its composition as in section sites 4-6 with light medium sand at the base with darker coarse sandy-gravelly intrabeds. A large lens of horizontally laminated fine to coarse sand, 24 m long and 2 m thick, ends subunit A3, with a sharp erosional surface to subunit A3. Two similar lenses of smaller scale, 6 to 10 m long and 40 cm thick, occur in the eastern part of subunit A1 (Fig. 15C). The bottom boulder-cobble member (A1) consists of massive, clast-supported cobble gravel, interbedded with beds and small sand lenses, sometimes deformed. Maximum boulder size is 80 cm, but with most common clast sizes between 15-20 cm. The top boulder-cobble member (A3) shows massive, crudely bedded boulder cobble gravel beds, some with open frameworks and others with sandy-gravelly matrix infills.

Tectonic architecture and structural description. - The sediments of site 7 show brittle to ductile deformation structures of different scales (Fig. 15C). Yet another 'reverse Z- shaped' structure is present in the central part of the section. It forms a 30 m long thrust-fault, striking N35° and with a dip of 18° towards NW (Fig. 12). The thrust fault starts

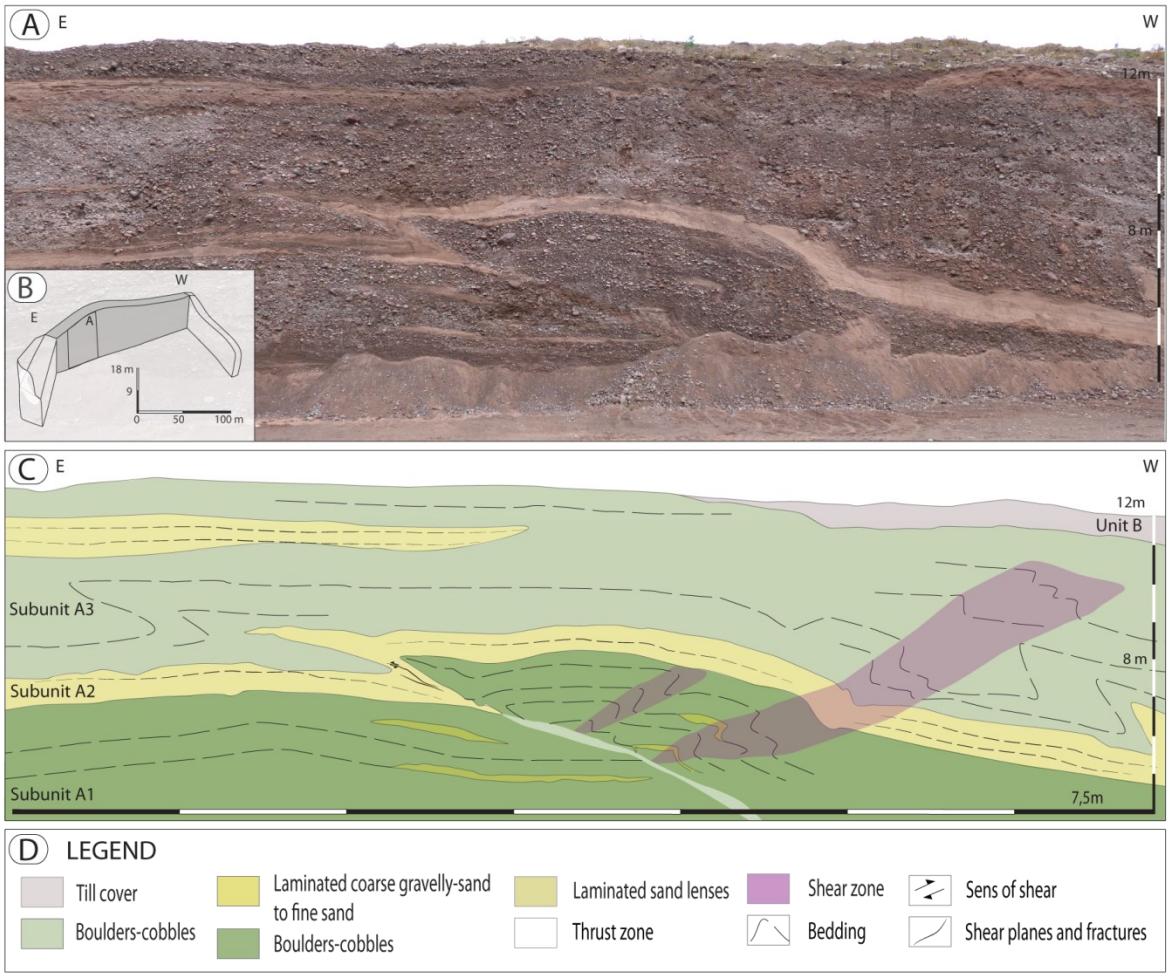

Fig. 15. Sediments and structures at site 7. (A) Photograph overview. (B) Position of section along the main section wall (gray shade) and covered area of photograph (A). (C) Section drawing of section site 7, including structural data. (D) Legend for section drawing.

below the pit base, cutting through subunit A1 as a thrust zone, crosses subunit A2 and continues into subunit A3. Subunits A1 and A3 display 'accumulation folding stacks' within a large shear zone to the right of the thrust (Fig. 15C). Small sand lenses within subunit A1 exhibit box folds with their hinges also part of this 'accumulation fold stacks' system. (Fig. 15C) The shear zones indicated in site 7 sediments could be associated to back thrusting, to conjugated shear zones or even to back thrusting kinking.

5.5.5. Combined glaciotectonic interpretations, sites 4, 5, 6 and 7 (unit A)

All sites (4-7) along section 2 suggest that the documented glaciotectonic deformation is from one deformational event, penetrating the whole sediment sequence (subunit A1-A3). From trends of fault/thrust planes and their dips (Fig. 12) it is concluded that the glaciotectonic stress at this deformation was from the WNW, which is oblique to the N-S trend of the Västerdalen valley.

The deformations revealed in section 2, with large-scale thrusts and folds, occur not only in the more fine-grained unit A2 sediment but also in the extremely coarse-grained unit A3 sediments. Such sediments will naturally have high shear strengths and thus also would require very high shear stresses to deform in this manner (Hart & Boulton 1991). However, if high pore-water pressure would be at hand, then strength of the sediment would be reduced as shear strength builds from effective stress (σ_n'; i.e. total normal stress reduced by pore-water pressure). High subglacial pore-water pressure would, especially in coarse-grained sediment, normally dissipate towards the ice margin. However, if proglacial permafrost is at hand sealing off the aquifer, then high pore-water pressure could be maintained far outside an ice margin. It would facilitate glaciotectonic work in submarginal to proglacial sediment, as has been described by, e.g., Moran (1971) and Aber *et al.* (1989) at formation of thrust block moraines.

The deformation as such cannot be dated, but the deformational events - without any age constraints - could either be tied to the same glacier whose meltwater deposited the sandur in front of it and that later deformed it during over-riding or that the deformation took place in sediment deposited during

an older glacial/deglacial phase that cannot be tied to the deformational event. The only existing age constraints are the above mentioned preliminary OSL ages. They suggest deposition of the sandur sediments in pre-Saalian times and that the covering till was deposited during the LGM deglaciation of the area. If a pre-Saalian age for the sandur sediment emplacement will be confirmed with the new set of pending OSL datings, the deformation would thus either also be of pre-Saalian age, or could be from any of the following Saalian or Weichselian glaciations over the Fiskarheden site. But with the exclusion of the Late Weichselian deglaciation as the direction of deformation in Fiskarheden does not concur with its ice-flow direction.

From the succession of mapped events it is suggested that the deformation started in the pro-glacial area of an advancing ice margin from the WNW. This is irrespective if the sandur was deposited in front of the advancing glacier margin, or deposited before that glacial event. During this advance, induced stresses exceeded the internal strength of the sandur sediments. It is suggested that high pore-water pressures, which might have been elevated due to proglacial permafrost in the upper parts of the coarse-grained sandur sediments, critically reduced effective stresses, meaning low sediment shear strength, and enhanced the substratum strain. This beginning-stage deformation might have been due to pushing from the rear or just due to the lateral glaciostatic stress gradient forwarded from the interior of the glacier towards its margin (Aber *et al.,* 1989).

Some 'piggy back-like thrusts' or 'stacked thrust blocks' could result from such stresses in an early stage and later overridden. In that case thrust faults were initiated in a gradual order, meaning the first to develop were those closest to the margin, and so on.

When ice advanced towards the ESE, irrespective if the Fiskarheden sandur was deposited during this advance in the proglacial area, or if being pre-existing, the sediment eventually became subglacial and simple shearing could occur continuously. The continuation of this deformation could have happened along two possible lines of processes: (i) ductile folding appeared in a very early stage, but was subsequently followed by brittle-ductile thrust failure within the subunit A2 sand, cutting up-section through the bouldery-cobbely beds of subunits A3 as fault-propagation-folds or, (ii) fault-propagation -folding occurred from the start and acted similarly to (i), but in time co-occurrence of faulting and folding. The fault-propagation-folding model of Brandes & Le Heron (2010) can possibly be used as correlative to the tectonic evolution at Fiskarheden. However, their models did not take pore-water pressure under consideration, but otherwise their simulations fit in terms of kinematic and internal features of what has been found in Fiskarheden.

As expressed by many authors (Rotnicki 1976; van der Wateren 1985; Aber *et al.* 1989; Williams *et al.* 2001) and what is often concluded from field work: glaciotectonics are most likely to develop at the ice margin where the ice has the steepest gradient and hence the highest lateral pressure gradient. Infra-marginal warm-based conditions are also known for releasing large amounts of water (encapsulated water mainly) which might have enhanced the glaciotectonism due to high porewater of the sediments (van der Wateren 1985).

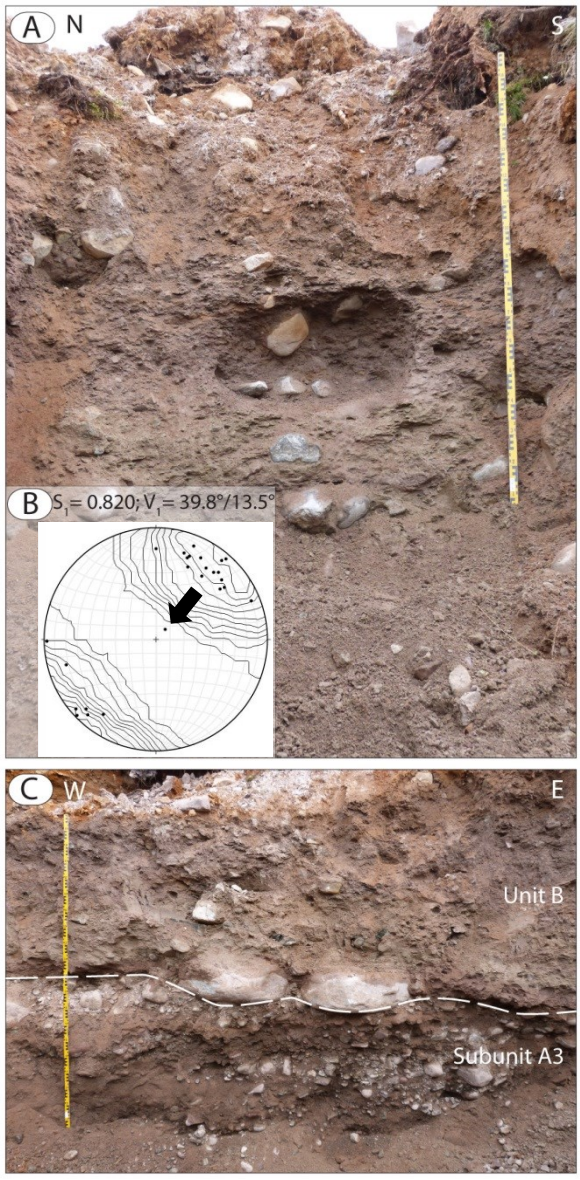

Fig. 16. Site 8 (Fig. 4), a test pit, 3 m deep, dug down from the original ground surface, c. 150 m behind the main section wall, though unit B diamict and into underlying subunit A3 sandur sediments. (A) Overview of site 8. (B) Clast fabric for site 8 diamicton. Data plotted on Schmidt equal-area lower-hemisphere projection and contoured according to the Kamb method at 2 σ intervals. Calculated strongest eigenvector (V_1) and normalized eigenvalue thereof (S_1) are shown, as well as interpreted ice flow direction (black arrow). (C) Close up of the E-W trending wall at site 8, showing the contact and 'clast pavement' between subunit A3 and overlying unit B. The contact is indicated with a white dashed line.

All thrusts and folds recorded at Fiskarheden are suggested to have been initiated almost simultaneously, enhanced to their formation by high-pressure water lubrication during the early phases of deformation. Folds and thrusts could have provided natural routes for the release of encapsulated meltwater or groundwater under high pressure, as suggested by Benediktsson *et al.* (2008). The glaciodynamic stress enhanced the shearing along the ice-bed interface, while the glaciostatic pressure enhanced an increase of the pore-water pressure (Benn & Evans, 2010), allowing the ductile water-saturated system to gradually change towards a ductile-brittle system and even almost brittle system (i.e., the shear zones of sites 4 and 7, Figs. 11B and 15C).

The back thrusting kinks (Bucher *et al.,* 2003) documented in Fiskarheden are suggested to have formed either (i) during functioning fault-propagation-folding as a counter balance of the listric fault-propagation folds (Williams & Vann, 1987), (ii) when the counter stress was at its highest, meaning when each sediment stack pile acted as 'a wall' to the other during gradual thrust stacking or, (iii) during both. However, not unimportant during the glaciotectonic deformation at Fiskarheden is the topographic situation; the sandur sediments are situated on the eastern flank of the N-S directed, deeply incised Västerdalälven valley (Fig. 1). The valley side and the sandur deposits along it would be situated close to perpendicular to an ice advancing from WNW and the

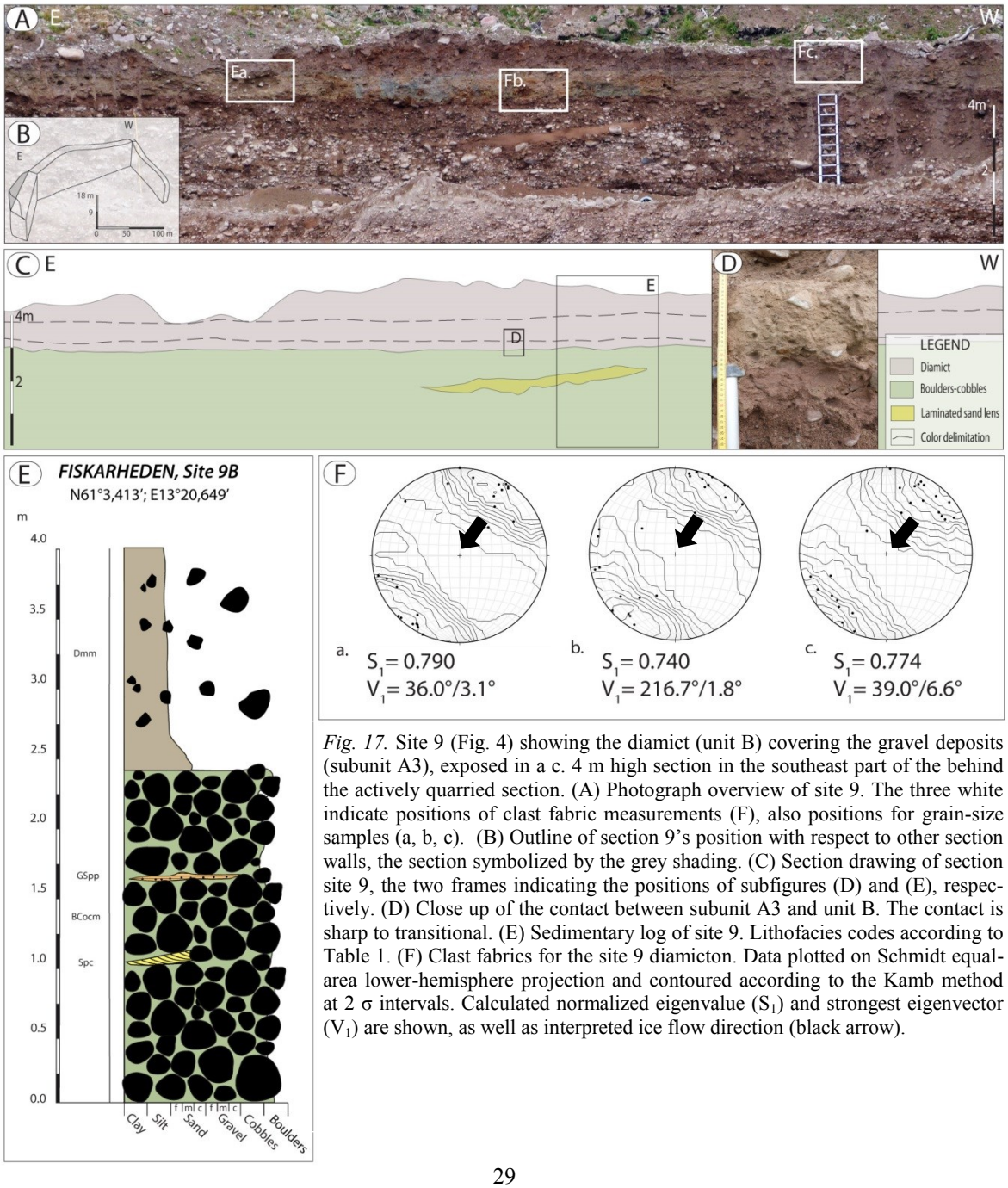

Fig. 17. Site 9 (Fig. 4) showing the diamict (unit B) covering the gravel deposits (subunit A3), exposed in a c. 4 m high section in the southeast part of the behind the actively quarried section. (A) Photograph overview of site 9. The three white indicate positions of clast fabric measurements (F), also positions for grain-size samples (a, b, c). (B) Outline of section 9's position with respect to other section walls, the section symbolized by the grey shading. (C) Section drawing of section site 9, the two frames indicating the positions of subfigures (D) and (E), respectively. (D) Close up of the contact between subunit A3 and unit B. The contact is sharp to transitional. (E) Sedimentary log of site 9. Lithofacies codes according to Table 1. (F) Clast fabrics for the site 9 diamicton. Data plotted on Schmidt equal-area lower-hemisphere projection and contoured according to the Kamb method at 2 σ intervals. Calculated normalized eigenvalue (S_1) and strongest eigenvector (V_1) are shown, as well as interpreted ice flow direction (black arrow).

valley side would act like a steep 'upslope wall' to glacier flow that possibly triggered the further evolution of the glaciotectonic deformation.

5.6. The covering diamict (unit B)

The diamict draping the glaciofluvial sediments was studied in a section c. 150 m south of the active quarry (site 8, Fig. 4) and along a section parallel but c. 10 m behind the quarried eastern pit wall (site 9, Fig. 4)

5.6.1. Site 8

Sedimentary composition. - The small test pit exposed 1.6 m of diamict (unit B) with a sharp contact with subunit A3 sediment (Figs. 16A and C). Unit B is composed of a massive, matrix-supported sandy diamict. Maximum clast size of the diamict in the section wall is 40 cm. A clast fabric analysis was made in the diamict70 cm above its basal contact to subunit A3 (Fig. 16A). Plotting of this reveal a unimodal, clustered fabric shape with a strong preferred clast axis orientation (S_1 = 0.820; V_1 = 39.8°/13.5°) (Fig. 16B). The V_1-axis orientation suggests a stress transfer from NE at deposition of the unit B diamict.

5.6.2. Site 9

Sedimentary composition. - The section wall is 4 to 4.5 m high and 11 m wide, trending N-S (Figs. 17A and B), documented in a log for the central part (Fig. 17E). Unit B overlies subunit A3 with a sharp to transitional contact (Fig. 17D). The section wall at the logged site is 4 m high (Fig. 4) and shows 2.1 m of subunit A3 boulder-cobble beds interbedded with two sand lenses, one with 30 cm cross bedded sand and the other with 10 cm of gravelly sand. When the contact with unit B is not sharp, this contact is transitional over c. 10 cm in which more rounded gravel and cobble clasts from subunit A3 are seen to be mixed with the diamict. The upper part of unit B is a matrix-supported, massive sandy to gravelly-sandy diamict. The clast content is medium to high with maximum particle sizes of 40 cm. Plots of performed clast fabric analyses (3) show unimodal, clustered fabric shapes with strong preferred clast axis orientations, two of them with moderately low dips (3° and 7°) towards N36° and N39°, and the third with a low dip towards 217° (Fig. 17F). S_1 values are between 0.740 and 0.790. They all suggest a NE/ NNE to SW/SSW stress transfer.

5.6.3. Sedimentological interpretation of sites 8 and 9 (unit B)

The depositional settings of the unit B diamict represent a sediment wedge of traction till, as suggested from its massive appearance and quite high strengths in preferred orientation of clasts, and suggesting the same stress transfer direction at the depositional ice-bed interface. The deposited till possibly cover the whole process spectrum from classic clast/matrix lodging to deformation of sediments below the ice-bed interface (definitions according to Benn and Evans 2010), the latter as indicated by the sometimes transitional contact between till and sandur sediment, suggesting incorporation of sandur sediment with the debris released at the bed contact in its lower part. As suggested from the fabric results, the deposition of unit B till did not coincide with the documented large-scale deformation of the underlying sandur sediments; the clast fabrics of the unit B till suggest an ice-flow direction during its emplacement from NE whereas the deformational structures with thrusts and folds in unit A is from the NW. Unit B must thus be from a later glacial stage over the area, and is consistent with the LGM deglacial direction over NW Dalarna, as suggested by, e.g. Lundqvist (1951) and Kleman (1990) from their studies of ice flow indicators.

6. Tectonic models in time evolution scale

Based on the observations of tectonic structures at Fiskarheden and with comparisons with similar features in the literature, an interpretative sequential model is proposed (Figs. 18, 19 and 20). The model includes four evolutionary phases, and is presented in two different scenarios (Figs. 18 and 19). The first scenario (Figs. 18B and 19) shows a deformation which occurred as the glacier expanded over is proglacially deposited sandur sediment, i.e. the deformation is in time closely related to its primary emplacement, while the second scenario (Figs. 18C and 19) of deformation is not coupled to sandur emplacement, i.e. the sandur was preexisting.

Deformation scenario one. - The Fiskarheden succession was deposited in proglacial proximal position to an advancing glacier as suggested by its resemblance to Trollheim or Scott sandur succession types (subunits A1 and A3) (Fig. 18). But as also indicated from the internal architecture there was some dramatic changes in depositional environments on the braid-plain system as suggested from the transfers between subunits A0/A1, A1/A2 and A2/A3. The bouldery-cobbely succession of subunit A1 was interrupted by – and most probably preceded by (subunit A0) – outburst event(s), as indicated by the sharpness of the contacts between subunit A1, A2 and A3 and the eventuality of subunit A0 as a correspondence to subunit A2. The sandur was water saturated and had a braided rivers pattern with bars and channels fluctuating along its surface.

As the ice margin advanced it induced glaciostatic as well as glaciodynamic and lateral stresses (cf. section 2.2 for more details) into its foreland (Fig. 18B). When these stresses exceeded the shear strength of the sediments deformation was initiated. The deformation is presumed to have started with compression of the syn-deposited sandur sediment strata, resulting in the formation of open folds that subsequently developed into asymmetric folds (Fig. 18B). Simultaneously, these folds sheared

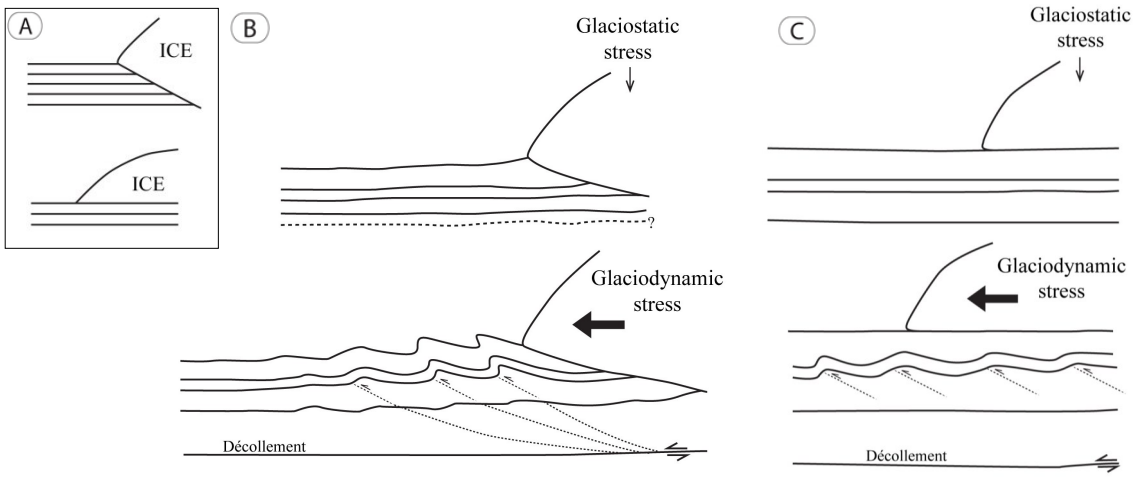

Fig. 18. (A) The two proposed scenarios of deformation of the Fiskarheden sandur, further developed in panels B and C. (B) Scenario 1; the sandur succession was deposited in a proglacial proximal position to an advancing glacier, followed by proglacial/subglacial deformation at glacier over-riding. Ice margin advanced induced glaciostatic as well as glaciodynamic and lateral stresses (cf. section 2.2 for more details) into its foreland. When these stresses exceeded the shear strength of the sediments deformation was initiated. The deformation is presumed to have started with the compression of the syn-depositing sandur sediments strata, resulting in the formation of open folds that subsequently developed into asymmetric folds. A presumable surface of décollement was formed coincidently. (C) Scenario 2; sandur deposition was uncoupled to its later deformation i.e. pre-existing. As an ice margin approached the preexisting sediments, deformation might have started already in near-marginal position, followed by subglacial deformation at glacier over-riding.

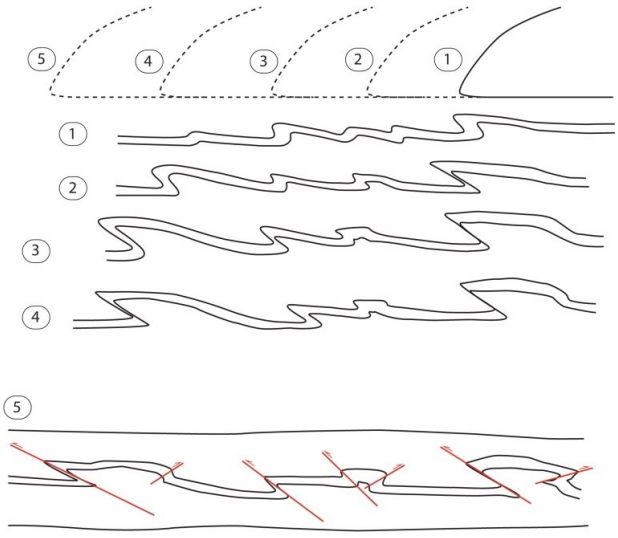

Fig. 19. Reconstructed sequential deformational phases (1-5), showing progression and evolution of ductile and brittle deformation of the Fiskarheden sandur sequence (valid for both deformational scenarios in Fig. 18). For further explanation, see text.

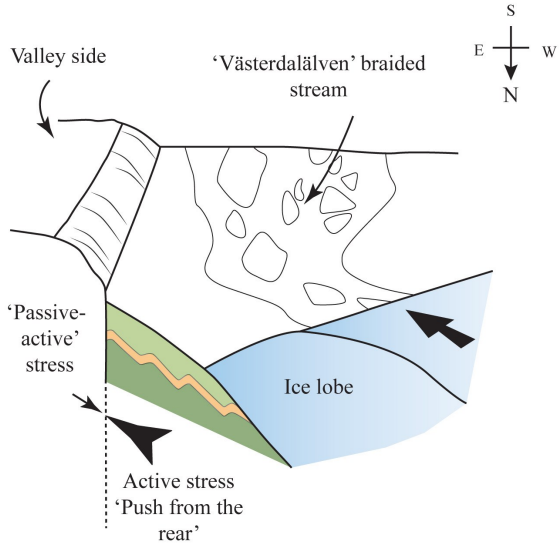

Fig. 20. Hypothetical palaeoenvironmental reconstruction of the Västerdalälven valley as a glacier margin advanced from WNW, which is oblique to the N to S valley trend in which the sandur was deposited (see text for more details). The eastern valley side might in this situation acted as 'blocking wall' initiating and enhancing counter stresses facilitating the proglacial/subglacial deformation of the sediments.

over the underlying sediments, as indicated by the box folds. These folds are verging east-southeast with approximately north to south oriented fold axes as a result of pressure application from the west-northwest. It is also been presumed that a surface of décollement was created coincidently and at least 20 m beneath the ice-bed interface since such have not been observed in the exposed part of the section.

As the deformation progressed, folds kept on getting sheared (Fig. 19). During further propagation of the deformation the distal part of the folds is assumed to have become broken by fault-propagation folds, while the rest of the sediments became simultaneously subject also to brittle deformations (i.e. shearing along both normal and thrust faults). The back thrust kinks should have been created during functioning fault-propagation-folding as a counter balance of the listric fault-propagation folds or when

the counter stress was at its highest, meaning when each sediment stack pile acted as 'a wall' to the other during gradual thrust stacking.

At the last stage of the deformation the glacier overrode the entire sandur system enhancing some subglacial shearing (Fig. 19, phase 5).

Deformation scenario two. - In this scenario sandur deposition, as discussed above, was uncoupled to its later deformation. In this scenario the sandur sequence at Fiskarheden was thus pre-existing, deposited in conjunction to another glacial phase that later induced the observed deformation (Fig. 18C).

As the ice margin approached the preexisting sediments, deformation might have started already in near-marginal position (proglacial deformation similar to first scenario but over shorter time and intensity of the deformation scales) due to the forwards stress propagation (Fig. 18C). Within a continuum, the ice sheet kept on moving forward and shearing was directly enhanced below the ice-bed interface (Fig. 19, phase 1). The closer to that interface of the subglacially deforming shear zone, the more deformed the sediments could get. In a supposedly 30 m thick sandur sequence overridden by a glacier some few hundred meters thick, most deformation would take place at the ice-bed interface and gradually decrease downwards as suggested in the subglacial shear zone diagram of Benn and Evans (2010), their fig. 10.5b. The initially high porewater pressure, facilitating deformation, is suggested to have dissipated progressively and leading to a more brittle-type deformation in a later stage (Fig. 19, phase 4).

The order in which thrusts evolve is uncertain according to Benediktsson et al. (2010). However, as some thrust-folding movement start to wane, they might function as a 'blocking wall', initiating the formation of the following thrust. Such 'secondary thrusts' movements might also rework the system already in place in a more brittle way. In fact, as said before, when pore-water pressure decreases, the ductile-brittle system is pushed to a brittle failure at which cataclastic/mylonitic thrusts could have been formed. Back thrusting kinks were formed either (i) during the functioning listric faulting-folding system as a counter balance to the listric fault-propagation-folds or, (ii), when the counter stress was at its highest, meaning when each sediment stack acted as a 'blocking wall' to the other or, (iii) during both.

Another possible source for formation of a counter stress is (iv) the morphological situation with the Fiskarheden sandur sediments clinging to the eastern side of the N-S directed Västerdalälven valley, this situated oblique to the ice advance from WNW and thus possibly acting as a 'blocking wall' (Fig. 20).

Later (post-deformational) glacier overriding. - Performed clast fabrics in the till (unit B) on top of the Fiskarheden sandur sequence suggest an ice flow direction from NE at its emplacement, which concurs with the LGM ice flow direction at retreat over the area (Kleman 1990). The major glaciotectonic deformation of the underlying sandur sediments can, accordingly, not be tied to this overriding. However, it might have caused erosion of unit A sediment of unknown depth before deposition of the unit B till. As these glacial phases cannot be dated, it is an open question if the deformational phase from WNW was at the interception of the LGM ice sheet and its subsequent advance over the area, or if this deformation occurred during some earlier glaciation over the area. As suggested from the Kleman *et al*. (1992) study on glaciofluvial drainage channels on the nearby Transtrand Mountains there are several to choose from.

7. Conclusions

From the observations on the morphology and internal architecture of the Fiskarheden gravel pit and the comparative mapping of the surrounding area, the following conclusions are drawn:

- The exposures within the pit suggest a primary deposition of the coarse-grained sediment in an ice proximal braided stream (sandur) environment (Scott type facies association) predominated by vertical accretion of braid-bar sediments.

- The deposition of above was at least once interrupted by major melt-water out-burst(s), depositing thick unit(s) of m-scale sand across the entire braid-plain, after which vertical aggradation of coarse-grained braid bar sediments resumed.

- The exposed sediment show large-scale deformation with fault-propagation folding and also brittle deformation creating cataclastic/ mylonitic systems, all from the northwest. The deformation started in proglacial position as an ice margin came close and continued in its last phases as subglacial deformation; due to the very coarse nature of most of the sediment it is speculated that such deformation was made possible due to high pore-water pressures encapsulated in proglacial position by permafrost.

- The geomorphology of the Västerdalälven river valley, trending N-S, might have been a key factor for inducing counter stress at ice over-riding and therefore might have enhanced or even created back-kinking within the Fiskarheden sediments.

- The direction of the Fiskarheden glacial tectonics coincides with the NW-SE alignment of the dominating glacial geomorphic elements of NW Dalarna (streamlined terrain and ribbed

moraine) and that deviates from the last deglacial flow direction, which is from N-NNE.

- The deformation as such cannot be dated to any larger accuracy that it postdates the primary deposition of the sandur sediments, which by preliminary OSL dating is set to be pre-Saalian in age.

- Two deformational scenarios are presented; (i) either the sediments were deformed in conjunction with the same glacial advance that produced the proglacial sandur sequence (i.e. pre-Saalian) at glacial over-riding or, (ii) the deformation took place at a later glacial advance over the area. In the last case the sandur sediment could represent deglacial deposits from an earlier glacial event than that producing the deformation.

- The Fiskarheden sandur deposits are covered by a traction till deposited from NE/NNE. This direction, as shown in performed clast fabric analyses, conforms in direction to younger cross-cutting streamlined terrain to the older NW-SE system and is suggested to represent the LGM deglaciation phase over the area.

8. Acknowledgements

Many thanks first go to my supervisor Per Möller for opportunity to be part of this project. Thank you for supervising and supporting me all along this project. Along this Master project I have had many supporting people that I would like to also thank particularly, such as Jean-Pierre Brun and Ìvar Örn Benediktsson and Lena Håkansson who gave important inputs and advices on tectonics, glaciotectonics and glacial environments during the first and the last steps of the project. Special thanks go to Tom Dowling for constructive comments and discussions to improve the thesis. Much gratitude goes to Laurie Charrieau, Nathalie Van der Putten, Joaen Stamsnijder and Guillaume Fontorbe for support and amazing times here in Sweden. I thank Carolina Funkey, Helena Alexanderson, Helena Filipsson, Sofia Åkesson, Sara Kullberg and Alexandra Glommé for great help during my thesis work. Furthermore I thank Elodie Hamon and Tom Dowling's for advices, help and company during lab-work. Thanks also go to all the Master students, Sofia, Sara, Alexandra, Joaen, Victor, Joakim, Emilie, Ludvig, Bernhard, Helen, Henrik, Olof et al., PhD students and Post-Docs, Laurie, Nathalie, Carolina, Tom, Guillaume, Claire, Wim, Patrick, Florian A., Florian M., Lorraine, Wenxin et al., and staff of Lund University which gave me an amazing working atmosphere as well as unforgettable fun times and giving me the feeling I belong. I also thank the working team at the Fiskarheden quarry pit who gave important help during field work and shared this middle Sweden experience with me.

A very special thank to my friends, Joaen, Gema, Jens, Linh, Sofia, Nathalie, Guillaume, Etienne, Alexis, Elodie, Anne-Sophie, Sylvain, Jeanne, Fred and Fernanda… for being thoughtful and encouraging as well as providing plenty of fun.

From the bottom of my heart, enormous thanks to my grandparents, Thérèse and Arsène, and to my chosen family Marie-Theres and Hubert, Jean-Michel and Annick, Valérie and Rémi and Jackie and Mark for your help, constant support and for believing in me all along.

It has been a long and sinuous journey but definitely one of the most interesting and achieving one..!

9. References

Aber, J.S., Croot, D.G. & Fenton, M.M., 1989: *Glaciotectonic Landforms and Structures*. Kluwer, Dordrecht, 200 pp.

Alexanderson, H., Johnsen & T., Murray, A., 2010: Re-dating the Pilgrimstad Interstadial with OSL: a warmer climate and a smaller ice sheet during the Swedish Middle Weichselian. Boreas 39, 367–376.

Alley, R.B., Blankenship, D. D., Bentley, C. R. & Rooney, S. T., 1986: Deformation of till beneath ice stream B, West Antarctica. *Nature* 322, 57–59.

Allmendinger, R. W., Cardozo, N. C., and Fisher, D., 2013: Structural Geology Algorithms: Vectors & Tensors: Cambridge, England, *Cambridge University Press*, 289 pp.

Banham, P.H., 1988: Thin-skinned glaciotectonic structures. In: Croot, D.G. (Ed.), *Glaciotectonics: Forms and Processes* 21–25. Balkema, Rotterdam.

Blankenship, D. D., Bentley, C. R., Rooney, S. T. & Alley, R. B., 1986: Seismic measurements reveal a saturated, porous layer beneath an active Antarctic ice stream. *Nature* 322, 54–57.

Benn, D.I. & Evans, D.J.A., 2010. *Glaciers and Glaciation* 734 pp. Arnold, London

Benediktsson, Í.Ö., Möller, P., Ingólfsson, O., van der Meer, J.J.M., Kjaer, K.H. & Krüger, K., 2008: Instantaneous end moraine and sediment wedge formation during the 1890 glacier surge of Brúarjökull, Iceland. *Quaternary Science Reviews* 27, 209–234.

Benediktsson, Í.Ö., Schomacker, A., Lokrantz, H. & Ingólfsson, Ó., 2010: The 1890 surge end moraine at Eyjabakkajökull, Iceland: a re-assessment of a classic glaciotectonic locality. *Quaternary Science Reviews* 29, 484–506

Boothroyd, J. C. & Ashley, G. M., 1975: Processes, bar morphology, and sedimentary structures on braided outwash fans, northeastern Gulf of Alaska. In: A. V. Jopling & B. C. McDonald (Editors), *Glaciofluvial and Glaciolacustrine Sedimentation* 23, 193–222. Society of Economic Paleontologists and Mineralogists.

Boulton, G.S., 1979: Processes of glacier erosion on different substrates. *Journal of Glaciology* 23, 15–38.

Boulton, G.S., 1982: Subglacial processes and the development of glacial bedforms. In: Davidson-Arnott, N.W., Fahey, B.D. (Eds.), Research in glacial, glacio-fluvial and glacio-lacustrine systems, 1-32. Proceedings of the 6th Guelph Symposium on geomorphology, 1980. Geo Books Norwich.

Boulton, G.S., 1987: A theory of drumlin formation by subglacial sediment deformation. In: Menzies, J., Rose, J. (Eds.), Drumlin Symposium, 25-80. A. A. Balkema, Rotterdam.

Boulton, G.S. & Jones, A.S., 1979: Stability of temperate ice caps and ice sheets resting on beds of deformable sediment. *Journal of Glaciology* 24, 29–43.

Boulton, G.S. & Hindmarsh, R.C.A., 1987: Sediment deformation beneath glaciers: Rheology and geological consequences. *Journal of Geophysical Research* 92(B9): 9059–9082.

Boulton, G.S., Smith, G.D., Jones, A.S. & Newsome, J., 1985: Glacial geology and glaciology of the last mid-latitude ice sheets. *Journal of the Geological Society*, London 142, 447-–474.

Brandes, C. & Le Heron, D.P., 2010: The glaciotectonic deformation of Quaternary sediments by fault-propagation folding. *Proceedings of the Geologists' Association* 121, 270–280.

Bucher, S., Schmid, S.M., Bousquet, R.& Fügenschuh, B., 2003: Late-stage deformation in a collisional orogen (Western Alps): nappe refolding, back-thrusting or normal faulting? *Terra Nova* 15, 109–117.

Croot, D.G., 1987: Glacio-tectonic structures: a mesoscale model of thin-skinned thrust sheets? *Journal of Structural Geology* 9, 797–809.

Denton, G.H. & Hughes, T.J., 1981: The Last Great Ice Sheets. *Wiley*, New York

Dowling, T.P.F., Alexanderson, H. & Möller, P., 2013: The new high resolution LiDAR digital height model (‘Ny Nationell Höjdmodell’) and its application to Swedish Quaternary geomorphol-ogy. GFF 135:2, 145–151.

Eyles, N., Eyles, C. H., Miall, A. D., 1983: Lithofacies types and vertical profile models; an alternative approach to the description and environmental interpretation of glacial diamict and diamictite sequences. Sedimentology 30, 393–410.

Hardy, S. & Poblet, J. 1995: The velocity description of defor-mation. Paper 2: Sediment geometries associat-ed with fault-bend and fault-propagation-folds. *Marine and Petroleum Geology* 12, 165–176.

Hart, J.K. & Boulton, G.S., 1991: The interrelation of glaciotectonic and glaciodepositional processes within the glacialenvironment. *Quaternary Science Reviews* 10, 335–350.

Helmens, K. F., 2009: Early MIS 3 glacial lake evolution, ice-marginal retreat pattern and climate at Sokli (northeastern Fennoscandia). Quaternary Science Reviews 28, 1880–1894.

Helmens. K.F., Räsänen, M. E., Johansson, P. W., Junger, H. & Korjonen, K., 2000: The last Interglacial-Glacial cycle in NE Fennoscandia: a nearly continuous record from Sokli (Finnish Lapland). *Quaternary Science Reviews* 19, 1605–1623.

Helmens, K.F., Bos, J.A.A., Engels, S., Van Meerbeeck, C.J., Bohncke, S.J.P., Renssen, H.,

Heiri O., Brooks, S.J., Seppä, H., Birks, H.J.B. & Wohlfarth B., 2007: Present day temperatures in northern Scandinavia during the last deglaciation. *Geology* 35(11), 987–990.

Helmens, K.F. & Engels, S., 2010: Ice-free conditions in eastern Fennoscandia during early Marine Isotope Stage 3: lacustrine records. *Boreas* 39, 399–409.

Hjelmqvist, S. 1966: Beskrivning till bergrundskarta över Kopparbergs län, *Sveriges Geologiska Undersökning* 40, 217 pp.

Hättestrand, M., 2007: Weichselian interstadial pollen stratigraphy from a Veiki plateau at Rissejauratj. *GFF* 129, 287–294.

Hättestrand, M. & Robertsson, A-M., 2010: Weichselian interstadials at Riipiharju, northern Sweden – interpretation of vegetation and climate from fossil and modern pollen records. *Boreas* 39, 296–311.

Hobbs, B. E., Means, W. D. & Williams, P. F., 1976: An Outline of Structural Geology. *Wiley*, New York.

Kleman, J. 1990: On the use of glacial striae for reconstruction of paleo-ice sheet flow patterns - with application to the Scandinavian ice sheet. *Geografiska Annaler* 72A (3-4), 217–236.

Kleman, J., Borgström, I., Robertsson, A.-M. & Liljesköld, M., 1992: Morphology and stratigra -phy from several deglaciation events in the Transtrand mountains, western Sweden. *Journal of Quaternary Science* 7, 1–16.

Kleman, J. & Glasser. N.F., 2007: Subglacial Thermal Organization (STO) of Ice Sheets. *Quaternary Science Reviews* 26, 585–597.

Kleman, J., Hättestrand, C., Borgström, L., Stroeven, A.,1997: Fennoscandian palaeoglaciology reconstructed using a glacial geological inversion model. *Journal of Glaciology* 43, 283–299.

Kleman, J. & Hättestrand, C., 1999: Frozen-bed Fennoscandian and Laurentide ice sheets during the Last Glacial maximum. *Nature* 402, 63–66.

Kleman, J. & Stroeven, A.P., 1997: Pre glacial surface remnants and Quaternary glacial regimes in north-western Sweden. *Geomorphology* 19, 35 –54.

Lagerbäck, R., 1988a: The Veiki moraines in northern Sweden – widespread evidence of an Early Weichselian deglaciation. *Boreas* 17, 469-–486.

Lagerbäck, R., 1988b: Periglacial phenomena in the wooded areas of north Sweden – relicts from the Tärendö interstadial. *Boreas* 17, 487–499.

Lagerbäck, R. & Robertsson, A-M., 1988: Kettle holes – stratigraphic archives for Weichselian geology and palaeoenvironment in northernmost Sweden. *Boreas* 17, 439-–468.

Lapworth, C., 1885: The highland controversy in British Geology, its causes, course and consequences. *Nature* 32, 558–9.

Ljungner, E., 1949: East-West Balance of the Quaternary Ice Caps in Patagonia and Scandinavia. *Bulletin of the Geology Instistute of Upsala* 33, 11–96.

Lundqvist, G., 1951: Beskrivning till jordartskarta över Kopparbergs län. *Sveriges Geologiska Undersökningar* 21, 213pp.

Lundqvist, J., 1969b: Beskrivning till jordartskarta över Jämtlands län. *Sveriges Geologiska Under -sökningar* 45, 418 pp.

Lundqvist, J., 1986: Late Weichselian glaciation and deglaciation in Scandinavia. In Sibrava, V., Bowen, D.Q. & Richmond, G.M. (eds), Quater -nary Glaciations in the Northern Hemisphere. *Quaternary Science Reviews* 5, 269–292.

Lunkka, J. P., Murray, A. & Korpela, K., 2008: Weichselian sediment succession at Ruuna, Finland, indicating a Mid-Weichselian ice-free interval in eastern Fennoscandia. *Boreas* 37, 234–244.

Lunkka, J. P., Saral, P. & Gibbard, P.L., 2015: The Rautavaara section, western Finnish Lapland, revisited – new age constraints indicate complex Scandinavian Ice Sheet history in northern Fennoscandia during the Weichselian Stage. *Boreas* 44, 68-–80.

Madsen, T. M. & Piotrowski, J. A. 2012: Genesis of the glaciotectonic thrust-fault complex at Halk Hoved, southern Denmark. *Bulletin of the Geological Society of Denmark* 60, 61–80.

Magilligan, F.J., Gomez, B., Mertes, L.A.K., Smith, L.C., Smith, N.D., Finnegan, D. & Garvin, J.B., 2002: Geomorphic effectiveness, sandur devel-opment, and the pattern of landscape response during jökulhlaups: Skeiðarársandur, southeast-ern Iceland. *Geomorphology* 44, 95–113.

Maizels, J.K., 1993a: Quantitative regime modelling of fluvial depositional sequences: application to Holocene stratigraphy of humid-glacial braid-plains (Icelandic sandurs). In: North, C.P. & Prosser, D.J. (Eds.), *Characterization of Fluvial and Aeolian Reservoirs*, vol. 73, 53–78. Geo-logical Society America Special Publication.

Maizels, J.K., 1993b: Lithofacies variations within sandur deposits: the role of runoff regime, flow dynamics and sediment supply characteristics. *Sedimentary Geology* 85, 299–325.

Maizels, J.K., 1997: Jökulhlaup deposits in proglacial areas. *Quaternary Science Review* 16, 793–819.

Mangerud, J., 1991a: The last interglacial/glacial cycle in northern Europe. In: Shane, L.C.K., Cushings, E.J. (Eds), *Quaternary landscapes*, p. 30–75. Minnesota University Press, 229 pp.

Mangerud, J., 1991b: The Scandinavian Ice Sheet

through the last interglacial/glacial cycle. In: B. Frenzel (ed): *Klima-geschichtliche Probleme der letzen 130 000 Jahre*, 451 pp. G. Fisher, Stuttgart, New York (Paleoklimaforschung Volume 1).

Mangerud, J., Gyllencreutz, R., Lohne, Ö. & Svendsen, J.I., 2011: Glacial history of Norway. In: Ehlers, J., Gibbard, P. L., Hughes, P.H. (Eds), *Quaternary Glaciations - Extent and Chronology - a closer look*, vol. 15, chap. 22, 279–298. Developments in Quaternary Science, .

Mark, D. M., 1973: Analysis of axial orientation data, including till fabrics. Geological Society of America Bulletin 84, 1369–1374.

Miall, A. D., 1977: A review of the braided-river depositional environment. *Earth Science Reviews* 13, 1–62.

Möller, P., Anjar, J. & Murray, A.S., 2013: An OSL-dated sediment sequence at Idre, west-central Sweden, indicating ice-free conditions in MIS 3. *Boreas* 42, 25–42.

Moran, S. 1971: Glaciotectonic structures in drift. *In:* Goldthwait, R.R. (ed.): *Till, a symposium*. Ohio State University Press, 127–148.

Nicholas, A.P. & Sambrook Smith, G.H., 1998: Relationships between flow hydraulics, sediment supply, bedload transport and channel stability in the proglacial Virkisa River, Iceland. *Geografiska Annaler* 80A, 111–122.

Pomerol, C., Lagabrielle,Y., Renard, M., & Guillot S., 2008: *Eléments de Géologie* Dunod, 13ème editon, 648pp.

Ramsay, J. G. & Graham, R. H. 1970: Strain variation in shear belts. *Canadian Journal of Earth Sciences* 7, 786–813.

Renineck, H.-E, Singh, I.B., 1975: Depositional Sedimentary Environments. Springer-Verlag, Berlin. 439 pp.

Rotnicki, K., 1976: The theoretical basis for and a model of the origin of glaciotectonic deformations. *Quaestiones Geographicae* 3, 103–139.

Russell, A.J. & Marren, P., 1999: Proglacial fluvial sedimentary sequences in Greenland and Iceland: a case study from active proglacial environments subject to jökulhlaups. In: Jones, A.P., Tucker, M.E. & Hart, J.K. (Eds.), *Q.R.A. Technical Guide Number 7*, 171–208. Quaternary Research Association, London.

Rust, B. R. 1972: Pebble orientation in fluvial sediments. *The Journal of Sedimentary Petrology* 42, 384–388

Salonen, V.P., Kaakinen, A., Kultti, S., Miettinen, A., Eskola, O.K. & Lunkka, J.P., 2008: Middle Weichselian glacial event in the central part of the Scandinavian Ice Sheet recorded in the Hitura pit, Ostrobothnia, Finland. *Boreas* 37, 38–54.

Spry, A., 1969: *Metamorphic Textures*. Pergamon Press. *Oxford* 8–559

Suppe, J. & Medwedeff, D.A., 1990: Geometry and kinematics of fault-propagation folding. *Eclogae Geologica Helveticae* 83, 409–454.

Svedlund, J.O., 2005: Moräntäckt isälvssediment sydost om Fiskarheden. SGU-rapport, 2005:8, 1–4.

Sverige geologiska undersökning 2015: Map generator. http://www.sgu.se/en/products/maps/map-generator/. Accessed 15.02.08.

Tikoff, B. & Fossen, H. 1993: Simultaneous pure and simple shear: the unifying deformation matrix. *Tectonophysics* 217, 267–283.

Ukkonen, P., Arppe, L., Houmark-Nielsen, M., Kjær, K. H., Karhu, J., 2007: MIS 3 mammoth remains from Sweden – implications for faunal history, palaeoclimate and glaciation chronology. Quaternary Science Reviews 26, 3081-3098.

Wateren, D. F. M. van der, 1985: A model of glacial tectonics, applied to the ice-pushed ridges in the Central Netherlands. *Bulletin of the Geological Society of Denmark* 34, 85–94.

Williams, P. F. & Rust, B. R. 1969: The sedimentology of a braided river. *Journal of Sedimentary Petrology* 39, 649–679.

Williams, G. & Vann, I., 1987: The geometry of listric normal faults and deformation in their hanging walls. *Journal of Structural Geology* 9, 789–795.

Williams, G.D., Brabham, P.J., Eaton, G.P. & Harris, C., 2001: Late Devensian glaciotectonic deformation at St Bees, Cumbria: a critical wedge model. *Journal of the Geological Society* 158, 125–135.

Wohlfarth, B., 2010: Ice-free conditions in Sweden during Marine Oxygen Istotope Stage 3? *Boreas* 39, 377–398.

Wohlfarth, B. & Näslund, J.-O., 2010: Fennoscandian Ice Sheet in MIS 3 – Introduction. *Boreas* 39, 325–327.

Wohlfarth, B., Alexanderson, H., Ampel, L., Bennike, O., Engels, S., Johnsen, T., Lundqvist, J. & Reimer, P., 2011: Pilgrimstad revisited – a multi-proxy reconstruction of Early/Middle Weichselian climate at a key site in central Sweden. *Boreas* 40, 211–230.

Zielinski, T. & Van Loon, A.J., 2003: Pleistocene sandur deposits represent braidplains, not alluvial fans. *Boreas* 32, 590–611.

Tidigare skrifter i serien "Examensarbeten i Geologi vid Lunds universitet":

414. Hjulström, Joakim, 2014: Bortforsling av kaxblandat vatten från borrningar via dag -vattenledningar: Riskanalys, karaktärise -ring av kaxvatten och reningsmetoder. (45 hp)
415. Fredrich, Birgit, 2014: Metadolerites as quantitative P-T markers for Sveconorwe -gian metamorphism, SW Sweden. (45 hp)
416. Alebouyeh Semami, Farnaz, 2014: U-Pb geochronology of the Tsineng dyke swarm and paleomagnetism of the Hartley Basalt, South Africa – evidence for two separate magmatic events at 1.93-1.92 and 1.88-1.84 Ga in the Kalahari craton. (45 hp)
417. Reiche, Sophie, 2014: Ascertaining the lithological boundaries of the Yoldia Sea of the Baltic Sea – a geochemical approach. (45 hp)
418. Mroczek, Robert, 2014: Microscopic shock-metamorphic features in crystalline bedrock: A comparison between shocked and unshocked granite from the Siljan impact structure. (15 hp)
419. Balija, Fisnik, 2014: Radon ett samhällsproblem - En litteraturstudie om geologiskt sammanhang, hälsoeffekter och möjliga lösningar. (15 hp)
420. Andersson, Sandra, 2014: Undersökning av kalciumkarbonatförekomsten i infiltra -tionsområdet i Sydvattens vattenverk, Vombverket. (15 hp)
421. Martin, Ellinor, 2014: Chrome spinel grains from the Komstad Limestone Formation, Killeröd, southern Sweden: A high-resolution study of an increased me -teorite flux in the Middle Ordovician. (45 hp)
422. Gabrielsson, Johan, 2014: A study over Mg/Ca in benthic foraminifera sampled across a large salinity gradient. (45 hp)
423. Ingvaldson, Ola, 2015: Ansvarsutredningar av tre potentiellt förorenade fastigheter i Helsingborgs stad. (15 hp)
424. Robygd, Joakim, 2015: Geochemical and palaeomagnetic characteristics of a Swedish Holocene sediment sequence from Lake Storsjön, Jämtland. (45 hp)
425. Larsson, Måns, 2015: Geofysiska undersökningsmetoder för geoenergisystem. (15 hp)
426. Hertzman, Hanna, 2015: Pharmaceuticals in groundwater - a literature review. (15 hp)
427. Thulin Olander, Henric, 2015: A contribu -tion to the knowledge of Fårö's hydrogeol-ogy. (45 hp)
428. Peterffy, Olof, 2015: Sedimentology and carbon isotope stratigraphy of Lower–Middle Ordovician successions of Slemmestad (Oslo-Asker, Norway) and Brunflo (Jämtland, Sweden). (45 hp)
429. Sjunnesson, Alexandra, 2015: Spårämnesförsök med nitrat för bedömning av spridning och uppehållstid vid återinfiltra -tionav grundvatten. (15 hp)
430. Henao, Victor, 2015: A palaeoenvironmental study of a peat sequence from Iles Kerguelen (49° S, Indian Ocean) for the Last Deglaciation based on pollen analysis. (45 hp)
431. Landgren, Susanne, 2015: Using calcein-filled osmotic pumps to study the calcification response of benthic foraminifera to induced hypoxia under *in situ* conditions: An experimental approach. (45 hp)
432. von Knorring, Robert, 2015: Undersökning av karstvittring inom Kristian -stadsslättens NV randområde och bedömning av dess betydelse för grundvattnets sårbarhet. (30 hp)
433. Rezvani, Azadeh, 2015: Spectral Time Domain Induced Polarization - Factors Affecting Spectral Data Information Con -tent and Applicability to Geological Char-acterization. (45 hp)
434. Vasilica, Alexander, 2015: Geofysisk karaktärisering av de ordoviciska kalkstensenheterna på södra Gotland. (15 hp)
435. Olsson, Sofia, 2015: Naturlig nedbrytning av klorerade lösningsmedel: en modellering i Biochlor baserat på en fallstudie. (15 hp)
436. Huitema, Moa, 2015: Inventering av föroreningar vid en brandövningsplats i Linköpings kommun. (15 hp)
437. Nordlander, Lina, 2015: Borrningsteknikens påverkan vid provtagning inför dimensionering av formationsfilter. (15 hp)
438. Fennvik, Erik, 2015: Resistivitet och IP-mätningar vid Äspö Hard Rock Laborato -ry. (15 hp)
439. Pettersson, Johan, 2015: Paleoekologisk undersökning av Triberga mosse, sydöstra Öland. (15 hp)
440. Larsson, Alfred, 2015: Mantelplymer - realitet eller *ad hoc*? (15 hp)
441. Holm, Julia, 2015: Markskador inom

skogsbruket - jordartens betydelse (15 hp)

442. Åkesson, Sofia, 2015: The application of resistivity and IP-measurements as inves -tigation tools at contaminated sites - A case study from Kv Renen 13, Varberg, SW Sweden. (45 hp)

443. Lönsjö, Emma, 2015: Utbredningen av PFOS i Sverige och världen med fokus på grundvattnet – en litteraturstudie. (15 hp)

444. Asani, Besnik, 2015: A geophysical study of a drumlin in the Åsnen area, Småland, south Sweden. (15 hp)

445. Ohlin, Jeanette, 2015: Riskanalys över pesticidförekomst i enskilda brunnar i Sjöbo kommun. (15 hp)

446. Stevic, Marijana, 2015: Identification and environmental interpretation of microtex -tures on quartz grains from aeolian sediments - Brattforsheden and Vittskövle, Sweden. (15 hp)

447. Johansson, Ida, 2015: Is there an influence of solar activity on the North Atlantic Oscillation? A literature study of the forcing factors behind the North Atlantic Oscillation. (15 hp)

448. Halling, Jenny, 2015: Inventering av sprickmineraliseringar i en del av Sorgen -frei-Tornquistzonen, Dalby stenbrott, Skåne. (15 hp)

449. Nordas, Johan, 2015: A palynological study across the Ordovician Kinnekulle. (15 hp)

450. Åhlén, Alexandra, 2015: Carbonatites at the Alnö complex, Sweden and along the East African Rift: a literature review. (15 hp)

451. Andersson, Klara, 2015: Undersökning av slugtestsmetodik. (15 hp)

452. Ivarsson, Filip, 2015: Hur bildades Bushveldkomplexet? (15 hp)

453. Glommé, Alexandra, 2015: 87Sr/86Sr in plagioclase, evidence for a crustal origin of the Hakefjorden Complex, SW Sweden. (45 hp)

454. Kullberg, Sara, 2015: Using Fe-Ti oxides and trace element analysis to determine crystallization sequence of an anorthosite -norite intrusion, Älgön SW Sweden. (45 hp)

455. Gustafsson, Jon, 2015: När började plattektoniken? Bevis för plattektoniska processer i geologisk tid. (15 hp)

456. Bergqvist, Martina, 2015: Kan Ölands grundvatten öka vid en uppdämning av de utgrävda dikena genom strandvallarna på Ölands östkust? (15 hp)

457. Larsson, Emilie, 2015: U-Pb baddeleyite dating of intrusions in the southeasternmost Kaapvaal Craton (South Afri -ca): revealing multiple events of dyke emplacement. (45 hp)

458. Zaman, Patrik, 2015: LiDAR mapping of presumed rock-cored drumlins in the Lake Åsnen area, Småland, South Sweden. (15 hp)

459. Aguilera Pradenas, Ariam, 2015: The formation mechanisms of Polycrystalline diamonds: diamondites and carbonados. (15 hp)

460. Viehweger, Bernhard, 2015: Sources and effects of short-term environmental changes in Gullmar Fjord, Sweden, inferred from the composition of sedimentary organic matter. (45 hp)

461. Bokhari Friberg, Yasmin, 2015: The paleoceanography of Kattegat during the last deglaciation from benthic foraminiferal stable isotopes. (45 hp)

462. Lundberg, Frans, 2016: Cambrian stratigraphy and depositional dynamics based on the Tomten-1 drill core, Falbygden, Väs-tergötland, Sweden. (45 hp)

463. Flindt, Anne-Cécile, 2016: A pre-LGM sandur deposit at Fiskarheden, NW Dalar -na - sedimentology and glaciotectonic deformation. (45 hp)

LUNDS UNIVERSITET

Geologiska institutionen
Lunds universitet
Sölvegatan 12, 223 62 Lund